



Hermann Stockinger

# Potential Analysis of Drive Train Efficiency in Plug-in Hybrid Electric Vehicles

Master Thesis

University of Technology Graz

Institute of Automotive Engineering

Head of Institute: Univ.-Prof. Dipl.-Ing. Dr.techn. Peter Fischer

Academic Supervision: Dipl.-Ing. Martin Ackerl

in cooperation with BMW Group

Company Supervision: Dr.-Ing. Georg Hepke

Graz, September 2015

This thesis is locked until September 2020.

## Statutory Declaration

I declare that I have authored this thesis independently, that I have not used other than the declared sources/resources, and that I have explicitly marked all material which has been quoted either literally or by content from the used sources.

Graz, \_\_\_\_\_

Date

\_\_\_\_\_

Signature

# Abstract

A potential analysis regarding efficiency of the subsystems IC engine and gearbox in plug-in hybrid electric vehicles was made. As an investigation platform a D-segment PHEV with a P2 drive train arrangement was selected. As a reference a conventional vehicle in same segment was modeled. Tests were conducted by applying different electric operating strategies in driving cycles NEDC and WLTC. The PHEV was tested in state-of-charge-minimum mode.

Concerning IC engine: First, operation in PHEV was analyzed. With the selected operating strategies, the operating time was reduced by more than 50 % compared to conventional vehicle. The average operating point was significantly shifting towards greater speeds and greater torques. Second, a calculation algorithm was developed, which allows quick and accurate comparative testing of IC engines with similar power quantities. Here a set of operating points builds the basis for consumption calculation. Third, the efficiency performance of different IC engine generations in the PHEV drive train was investigated.

Concerning gearbox a sensitivity analysis regarding the effect of friction torque reduction was made. It was found that in the hybrid drive train an increase of gearbox efficiency causes a significantly stronger CO<sub>2</sub> reduction than in the conventional one.

# Contents

<b>Abstract</b>	<b>iii</b>
<b>1 Introduction</b>	<b>1</b>
1.1 Motivations	1
1.2 Objectives	2
<b>2 State of the Art</b>	<b>5</b>
2.1 Types of Hybrid Electric Vehicles	5
2.2 Technologies on Market	6
2.2.1 Parallel Hybrid	6
2.2.2 Series Hybrid	7
2.2.3 Combined Hybrid	8
2.2.4 Power-Split Hybrid	9
<b>3 Methodology</b>	<b>11</b>
3.1 Energy Analysis	11
3.1.1 Longitudinal Vehicle Model	11
3.1.2 Subsystems	15
3.1.3 Power Flows in PHEV Drive Train	17
3.2 Vehicle Definition	22
3.2.1 Conventional Vehicle	23
3.2.2 Plug-in Hybrid Electric Vehicle	24
3.2.3 Subsystems	24
3.3 Use Case	26
3.3.1 Test Cycles	26
3.3.2 Procedure of Evaluation	28
3.3.3 Operating Strategy	30
3.4 Simulation Model	38
3.4.1 Longitudinal Vehicle Model	38

## Contents

3.4.2	IC Engine Model . . . . .	38
3.4.3	Gearbox Model . . . . .	41
3.5	Matlab Tool for Consumption Calculation . . . . .	42
3.5.1	Systematic of Calculation . . . . .	43
3.5.2	Reference Simulations as Basis of Valuation . . . . .	46
3.5.3	Ventus-Tool Environment . . . . .	48
3.5.4	Features and Benefits . . . . .	51
<b>4</b>	<b>Results</b>	<b>56</b>
4.1	IC Engine in Parallel Hybrid Vehicles . . . . .	56
4.1.1	Analysis of Operating Pattern . . . . .	56
4.1.2	Evaluation of IC Engine Generations . . . . .	60
4.2	Gearbox in Parallel Hybrid Vehicles . . . . .	69
4.2.1	Gearbox Operation . . . . .	69
4.2.2	Potential of Friction Reducing Measures . . . . .	71
<b>5</b>	<b>Conclusions</b>	<b>75</b>
	<b>Bibliography</b>	<b>77</b>

# List of Figures

1.1	CO <sub>2</sub> reduction potential of different electrification measures.	3
2.1	PHEV topology of Mercedes Benz S500 PHEV. . . . .	7
2.2	PHEV topology of BMW i3 REX. . . . .	8
2.3	PHEV topology of Mitsubishi Outlander PHEV. . . . .	9
2.4	PHEV topology of Toyota Prius PHEV. . . . .	10
3.1	External forces on a vehicle in motion. . . . .	12
3.2	Different modes of vehicle operation. . . . .	14
3.3	Efficiency consumption map of a SI IC engine. . . . .	16
3.4	Gearbox model for definition of transmission efficiency. . . . .	17
3.5	Simplified composition diagram of full parallel hybrid configuration. . . . .	18
3.6	Power flow for PHEV operating modes. . . . .	19
3.7	Energy management of parallel hybrid drive train. . . . .	20
3.8	Functionality of IC engine on-/off characteristic. . . . .	21
3.9	Topology of conventional vehicle. . . . .	23
3.10	Topology of PHEV vehicle. . . . .	25
3.11	Velocity Profile of NEDC. . . . .	28
3.12	Velocity Profile of WLTC. . . . .	29
3.13	Distribution of load points / 140kW SI IC engine operating in conventional vehicle in NEDC. . . . .	31
3.14	Distribution of load points / 140kW SI IC engine operating in conventional vehicle in WLTC. . . . .	32
3.15	SOC and ICE on-/off periods with eOS 1 in NEDC. & Distribution of load points / 140kW SI IC engine with eOS 1 in NEDC. . . . .	34

## List of Figures

3.16	SOC and ICE on-/off periods with eOS 2 in NEDC. & Distribution of load points / 140kW SI IC engine with eOS 2 in NEDC. . . . .	36
3.17	SOC and ICE on-/off periods with eOS 3 in WLTC. & Distribution of load points / 140kW SI IC engine with eOS 3 in WLTC. . . . .	37
3.18	Simulation composition diagram of longitudinal vehicle model. . . . .	39
3.19	Fuel flow consumption map of a SI IC engine. . . . .	40
3.20	Exemplary interactions between ICE characteristics and external influential factors for ICE operation. . . . .	43
3.21	Comparison of consumption calculation / Dymola simulation vs. derived Matlab calculation. . . . .	46
3.22	Systematic of Matlab consumption calculation. . . . .	49
3.23	Central control penal of Ventus-Tool. . . . .	51
3.24	Control panel for $\Delta$ -consumption map estimation. . . . .	54
4.1	CO <sub>2</sub> reduction over IC engine generations / 100kW SI IC engines in NEDC & WLTC. . . . .	64
4.2	CO <sub>2</sub> reduction over IC engine generations / 140kW SI IC engines in NEDC & WLTC. . . . .	67
4.3	CO <sub>2</sub> reduction over IC engine generations / 140kW CI IC engines in NEDC & WLTC. . . . .	70
4.4	Propulsion power and energy of PHEV vehicle in NEDC & WLTC. . . . .	72
4.5	CO <sub>2</sub> reduction over gearbox efficiency increase in NEDC & WLTC. . . . .	74

# List of Tables

2.1	Technical data of Mercedes Benz S500 PHEV. . . . .	7
2.2	Technical data of BMW i3 REX. . . . .	8
2.3	Technical data of Mitsubishi Outlander PHEV. . . . .	9
2.4	Technical data of Toyota Prius PHEV. . . . .	10
3.1	Technical specification of conventional vehicle. . . . .	23
3.2	Technical specification of plug-in hybrid vehicle. . . . .	24
3.3	Reference IC engines for simulation. . . . .	25
3.4	Reference gearbox for simulation. . . . .	26
3.5	Specifications of NEDC test cycle. [33] . . . . .	27
3.6	Duration of WLTC test cycle parts. . . . .	27
3.7	Specifications of WLTC testcycle. [35] [34] . . . . .	28
3.8	Motorization of conventional and PHEV vehicle. . . . .	48
4.1	IC engines range of operation / conventional vehicles in NEDC. . . . .	57
4.2	IC engines range of operation / PHEV with eOS 1 in NEDC. . . . .	58
4.3	IC engines range of operation / PHEV with eOS 2 in NEDC. . . . .	59
4.4	IC engines range of operation / conventional vehicles in WLTC. . . . .	59
4.5	IC engines range of operation / PHEV with eOS 3 in WLTC. . . . .	60
4.6	IC engine specification of 100 kW SI engine class / previous generation. . . . .	61
4.7	IC engine specification of 100 kW SI IC engine class / current generation (3-cylinder. . . . .	61
4.8	IC engine specification of 100 kW SI IC engine class / current generation (4-cylinder). . . . .	62
4.9	IC engine specification of 100 kW SI IC engine class / next generation. . . . .	62

## List of Tables

4.10	IC engine specification of 140 kW SI IC engine class / previous generation. . . . .	65
4.11	IC engine specification of 140 kW SI IC engine class / current generation. . . . .	65
4.12	IC engine specification of 140 kW SI IC engine class / next generation. . . . .	66
4.13	IC engine specification of 140 kW CI IC engine class / previous generation. . . . .	68
4.14	IC engine specification of 140 kW CI IC engine class / current generation. . . . .	69

# 1 Introduction

The introductory chapter describes how this work is embedded in a strategic decision making process for future plug-in hybrid electric vehicle concepts. In the following motivations are stated and the objectives of this work are defined.

## 1.1 Motivations

As worlds population booms, the global traffic volume is growing rapidly [31][4]. This is why global carbon dioxide emissions are increasing ever-faster and the ecological situation is worsening dramatically [7]. At the same time traffic is shifting more and more to urban areas. 2030 60 % of worlds population will live in megalopolis [32]. In these urban areas peoples growing demand for individual mobility on the one hand and the corresponding increase of traffic density on the other hand cause a contradictory development [4]. In order to lead Europe into a sustainable and competitive future, politicians are forced to take measures. For the automotive industry a highly relevant issue concerning these measures are the fleet emission limits.

Currently the average  $CO_2$  emission of registered new cars is  $130 \text{ g}_{CO_2}/\text{km}$  [1][19]. For 2021 the maximum of legal carbon dioxide fleet emission will be about  $95 \text{ g } CO_2/\text{km}$ . For 2025 a maximum of approximately  $75 \text{ g } CO_2/\text{km}$  will be allowed [1]. Figure 1.1 shows the  $CO_2$  reduction potential for different degrees of electrification. By improving the conventional drive train and by implementing hybrid functions without using energy sources other than fossil fuels, vehicles carbon-dioxide emission can be

## 1 Introduction

reduced by a maximum of 25 % [18]. This is too little to meet future emission restrictions. The electric range, powered by electric energy from the externally charged battery is labeled as zero emission mobility. Because of this the increase of electric range has a very strong impact on reducing carbon dioxide emissions. Hence, it is the plug-in electrification ratio which needs to be increased significantly in order to meet future legal requirements. European car manufacturers are increasingly investing in the Plug-in Hybrid Vehicle (PHEV) technology. PHEV technology is seen as an opportunity to significantly reduce carbon-dioxide emissions without changing the existing conventional drive train architecture totally [18]. From customers perspective pure electric drive in urban areas can be experienced without making compromises regarding range. Due to a smaller battery the charging time of plug-in hybrids is much shorter than of pure electric vehicles. Therefore plug-in hybrid vehicles are offering an efficient mobility solution for all regular demands and are considered as an all in one product. However, looking at long-term developments such as increasing carbon dioxide restrictions due to ecological changes and a future oil shortage on the one hand and a constantly increasing know-how for automotive electrification and decreasing costs of electric energy storage on the other hand, PHEVs are just seen as a transitional technology [8]. Nevertheless from today's perspective PHEVs are representing an attractive compromise [36][37].

In car industry it can be observed that plug-in hybrid technology is often based on an existing conventional architecture. Also the subsystems internal combustion (IC) engine (or ICE) and gearbox are often derived from conventional drive trains. This strategy minimizes costs as well as the required development effort [23]. The arising problem is that the specific usage of IC engines and gearboxes in plug-in hybrid topologies is significantly different.

### 1.2 Objectives

As already mentioned the PHEV is currently seen as a transitional technology. It enables a good compromise in terms of costs, efficiency and

## 1 Introduction

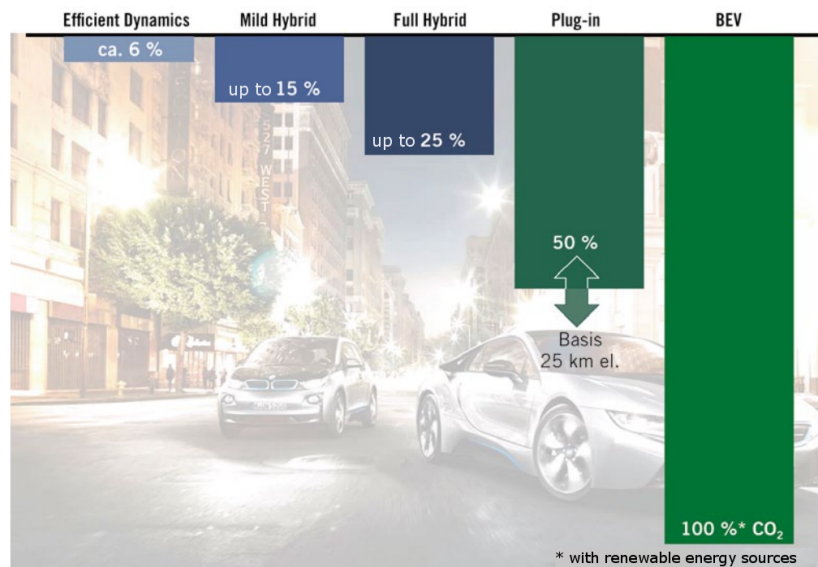


Figure 1.1: CO<sub>2</sub> reduction potential of different electrification measures. [18, p.57]

drive-ability. This is a reason why car manufacturers are often aiming to implement already existing elements in plug-in hybrid electric vehicles. Out of this situation a question comes up, which describes the central incentive of this work: *To what extent the plug-in hybrid vehicle can benefit from components, originally developed for conventional applications?* It is a central aim of this work to contribute to a solid base for strategic product decision making of car manufacturers. Therefore the specific use of these subsystems in PHEV topologies need to be analyzed.

The first matter of analysis is the PHEV-specific operation of IC engines. PHEV drive train control systems are deciding continuously whether the desired propulsion power gets delivered by the electric machine and/or by the IC engine. Generally it can be stated that the electric system is supplying propulsion power during phases of low-load and the IC engine is contributing for greater power demands. In contrast to operation in conventional drive trains IC engine ranges of operation in PHEVs are expected to be in areas of greater torque and greater speed. Hence, the understanding of this specific operation builds a basis for further analysis and therefore an elementary part of this work.

## 1 Introduction

The investigation of PHEV specific gearbox operation is another central issue. In section 3.2.2 the vehicle topology configured for this work is specified. Out of this parallel topology fundamental differences of gearbox operation is arising. The gearbox is not just transmitting propulsion power from the prime movers to the driving wheels but also other way round (recuperative energy flow). Here a general potential analysis concerning transmission efficiency is meant to build the base for following investigations.

## 2 State of the Art

Due to the mentioned CO<sub>2</sub> emission limits current OEMs<sup>1</sup> are more and more obliged to invest in emission reducing technologies. In general electrification is seen as a powerful way for increasing efficiency. Nevertheless pure electric vehicles are currently facing serious disadvantages such as the limited electric range and high costs of battery. As stated in the introduction, plug-in hybrid vehicles are seen as a possibility to combine the advantages out of two technologies [38]. However, for a successful implementation an efficient combination of the electric machine and the IC engine is crucial.

### 2.1 Types of Hybrid Electric Vehicles

During last years many different approaches were developed. Generally there are three main types for hybrid-electric vehicle classification:

- **Parallel hybrid:** The IC engine can be coupled mechanically with vehicle drive train. The electric motor can be operated parallel to IC engines drive train. Hence, the vehicle propulsion can be powered individually or simultaneously by IC engine and electric motor.
- **Series hybrid:** Just the electric motor is powering vehicle propulsion. The demanded electricity can be either supplied by the battery or by a generator which is driven by the IC engine.
- **Power-split and combined hybrid:** Power-split hybrids enable to divide the mechanical propulsion power into a mechanical and an electrical power path. A special case of this configuration is the combined hybrid. The combined configuration allows to operate the

---

<sup>1</sup>Original Equipment Manufacturer

## 2 State of the Art

PHEV in series as well as in parallel mode. Either the IC engine gets linked mechanically to the drive train, like the parallel hybrid, or the ICE is driving a generator for electrical energy supply, like the series hybrid. This functionality is achieved by two electric machines and a clutch in PHEV drive train.

[22, p.70 et sqq.][23, p.23 et sqq.]

As can be seen on market, the parallel hybrid platform, introduced in more detail in section 3.2.2, is representing a common configuration of European premium car manufacturers [24][28][26][12]. This is why this platform has been selected for the analysis of this work. [5]

In the next section a few representative concepts on market are introduced.

### 2.2 Technologies on Market

In the following the most important PHEV configurations on market are compared and discussed briefly.

#### 2.2.1 Parallel Hybrid

On market parallel hybrid configuration are represented by examples like Mercedes Benz S500 PHEV, Porsche Panamera PHEV, Audi A3 e-tron PHEV [24][28][26]. Exemplarily the S500 PHEV is described in more detail:

The Mercedes Benz S500 PHEV has been launched in June 2014. Figure 2.1 describes the systematic of its parallel hybrid drive train. This configuration of a PHEV propulsion system is considered as a solution which contributes positively to carbon dioxide emission reduction and still gives the opportunity to use current conventional vehicle architectures. Table 2.1 shows some technical data.

## 2 State of the Art

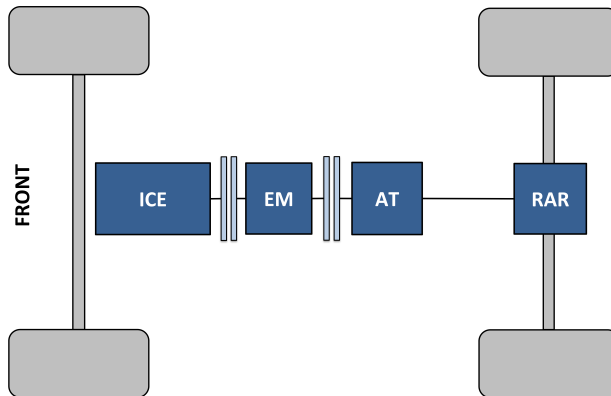


Figure 2.1: PHEV topology of Mercedes Benz S500 PHEV.

Table 2.1: Technical data of Mercedes Benz S500 PHEV. [24]

Unloaded mass	$m$	=	2095 kg
Pure electric range (NEDC)	$e - range$	=	33 km
Carbon Dioxide (NEDC)	$CO_2$	=	65 g $_{CO_2}$ /km
System power (maximum)	$P_{max}$	=	325 kW
System torque (maximum)	$T_{max}$	=	650 Nm
Driving performance	0 – 100 km/h	=	5,2 s

Technical data in this section is defined in the following way: The unloaded mass is given with respect to the DIN norm [9]. The electric range as well as the carbon dioxide emission value are determined by the NEDC testing procedure[33].

It can be observed that currently most parallel hybrid concepts on market have a pure electric range between 30 and 60 km [24][28][26][12].

### 2.2.2 Series Hybrid

On market series hybrid configuration is represented by examples like BMW i3 REX and Fisker Karma [10][20]. Exemplarily the i3 is described in more detail:

## 2 State of the Art

BMW i3 REX has been launched in Mai 2014. Figure 2.2 describes the systematic of its series hybrid drive train. Here the range issue of pure electric vehicles is compensated by the integration of a range extending IC engine (REX). The REX is directly coupled with a generator. It is a 2 cylinder spark ignited (SI) IC engine which is delivering 28 kW of power and 55 Nm of torque. Table 2.2 shows some technical data.

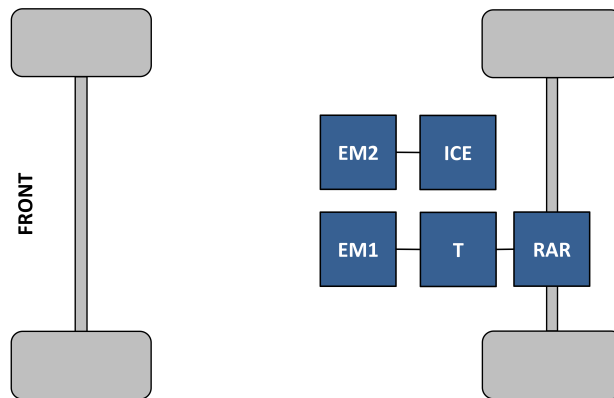


Figure 2.2: PHEV topology of BMW i3 REX.

Table 2.2: Technical data of BMW i3 REX. [10]

Unloaded mass	$m$	=	1390 kg
Pure electric range (NEDC)	$e - range$	=	170 km
Carbon Dioxide (NEDC)	$CO_2$	=	0 g $CO_2$ /km
Motor power (maximum)	$P_{max}$	=	125 kW
Motor torque (maximum)	$T_{max}$	=	250 Nm
REX power	$P_{REX}$	=	28 kW at 5000 rpm
REX torque	$T_{REX}$	=	55 Nm at 4300 rpm
Driving performance	0 – 100 km/h	=	7,9 s

### 2.2.3 Combined Hybrid

On market combined hybrid configuration is represented by examples like Mitsubishi Outlander PHEV (just the front axis drive) and the Chevrolet

## 2 State of the Art

Volt PHEV [25][16]. Exemplarily the Outlander PHEV is described in more detail:

The Mitsubishi Outlander PHEV has been launched in April 2014. Its drive train is assembled by a combined hybrid configuration at front axle and an electric drive at rear axle as shown in figure 2.3. The front axle is powered by the combustion engine as well as by an electric machine. Furthermore there is another electric machine directly coupled on the IC engine to act as a generator and enable series hybrid mode. Table 2.3 shows some technical data.

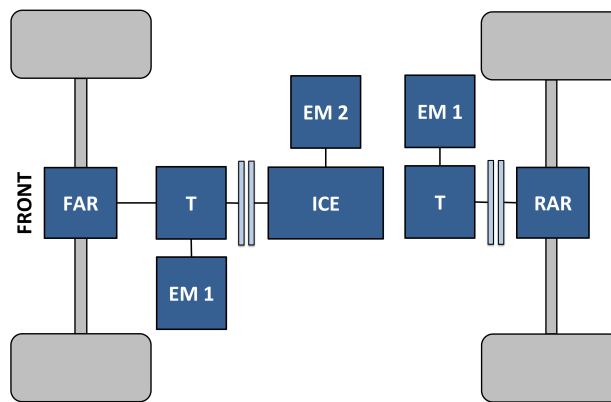


Figure 2.3: PHEV topology of Mitsubishi Outlander PHEV.

Table 2.3: Technical data of Mitsubishi Outlander PHEV. [25]

Unloaded mass	$m$	=	1810 kg
Pure electric range (NEDC)	$e - range$	=	52 km
Carbon Dioxide (NEDC)	$CO_2$	=	44 $g_{CO_2}/km$
System power (maximum)	$P_{max}$	=	190 kW
Driving performance	0 – 100 km/h	=	9,9 s

### 2.2.4 Power-Split Hybrid

On market examples for power-split hybrid configurations are Toyota Prius PHEV and Ford C-Max Energi [30][21]. Exemplarily the Prius PHEV

## 2 State of the Art

is described in more detail:

The current generation of Toyota Prius plug-in hybrid is on market since 2012. For this year the launch of the next generation is expected. The drive train is a power-split hybrid solution. As can be seen in figure 2.4 the drive train configuration of this car is representing another approach. The center of the propulsion system is a planetary transmission (PT). The two electric motors are able to adjust a continuous transmission ratio for the IC engine. Furthermore the electric motor 2 can be used to increase/decrease the IC engine torque. Hence, load-point shifting (LPS) (see section 3.1.3) and a continuous transmission ratio allow a very optimized operation of IC engine. Furthermore pure electric driving and a serial hybrid mode are possible. Table 2.4 shows some technical data.

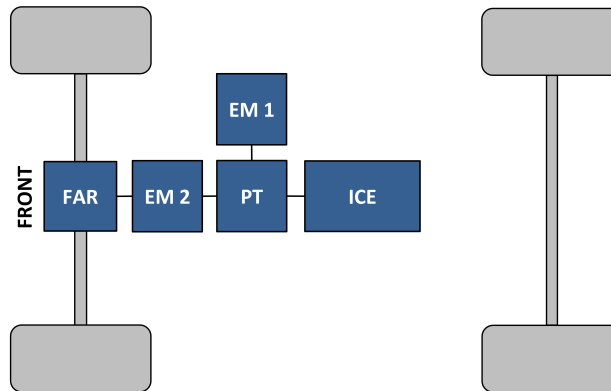


Figure 2.4: PHEV topology of Toyota Prius PHEV.

Table 2.4: Technical data of Toyota Prius PHEV. [30]

Unloaded mass	$m$	=	1420 kg
Pure electric range (NEDC)	$e - range$	=	23,4 km
Carbon Dioxide (NEDC)	$CO_2$	=	89 $g_{CO_2}/km$
System power (maximum)	$P_{max}$	=	134 kW
Driving performance	0 – 100 km/h	=	10,7 s

## 3 Methodology

In this chapter essential methods for investigation are introduced. First, a general analysis of acting forces on vehicle in motion is conducted, analytical assumptions for efficiency evaluation of IC engines and gearboxes are made and different operating modes with the corresponding power flows in parallel hybrid drive trains are stated. Second, the conventional and the plug-in hybrid vehicle are specified for analysis, use cases are defined and operating strategies are characterized. Third, the overall simulation model which is used as a basis for valuation is described and discussed. Here, the emphasis lies on the subsystems IC engine and gearbox. Finally, a developed Matlab calculation is introduced and explained.

### 3.1 Energy Analysis

In this section fundamentals of energy and efficiency analysis are prepared as a basis for the subsequent introduction of the Dymola simulation model and the Matlab calculation.

#### 3.1.1 Longitudinal Vehicle Model

To accelerate and decelerate a vehicle for following a test cycle, first, all resistance forces need to be compensated and second, the inertia of mass need to be overcome. Therefore the traction forces are transmitted in contact surfaces between tires and track. Figure 3.1 illustrates the mechanical system of vehicle during motion. For the longitudinal dynamic of vehicle, equation 3.1 represents the elementary correlation.

### 3 Methodology

- The term  $m_v \frac{d}{dt}v$  is representing vehicles inertia by the multiplication of mass times acceleration.
- $F_t$  is the propulsion force delivered by the prime mover minus the force for acceleration of every rotating elements and all friction in drive train.
- $F_a$  represents the aerodynamic drag force.
- $F_r$  stands for the rolling resistance force.
- $F_g$  describes the uphill driving force.
- $F_d$  is defined as a disturbance force which is summarizing every, not yet specified resistances.

Next the most important external forces are briefly discussed.

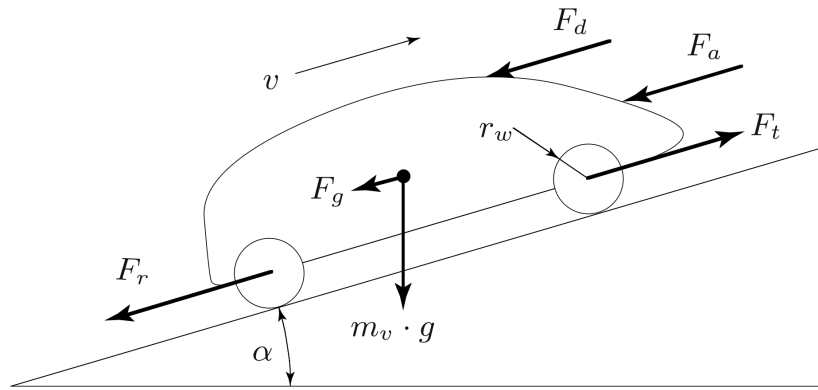


Figure 3.1: External forces on a vehicle in motion. [22, p.14]

$$m_v \frac{d}{dt}v(t) = F_t(t) - (F_a(t) + F_r(t) + F_g(t) + F_d(t)) \quad (3.1)$$

**Aerodynamic Drag Force** The aerodynamic friction acting on a moving vehicle is caused by two effects.

1. Pressure difference between front and rear.
2. Viscous friction of the air surrounding vehicles surface.

The aerodynamic friction force is strongly depending on velocity of airflow  $v$  in direction of vehicles longitudinal axis. Equation 3.2 is representing the physical law.  $F_a(v)$  is the force as applied in figure 3.1.  $\rho_a$

### 3 Methodology

is the density of the surrounding fluid (air).  $A_f$  is the projected frontal area of vehicle.  $c_d$  is the drag coefficient which is depending on the aerodynamic characteristic of vehicles body. [22, p.15]

$$F_a(v) = \frac{1}{2} \cdot \rho_a \cdot A_f \cdot c_d \cdot v^2 \quad (3.2)$$

**Rolling Resistance Force** The rolling resistance force  $F_r(v, p_t, \dots)$  as applied in figure 3.1 can be described with equation 3.3.  $c_r$  is the rolling friction coefficient which is depending on a quantity of variables. The vehicle speed  $v$  and tire pressure  $p_t$  are the most important influences.  $m_v$  is representing vehicles mass.  $g$  stands for the gravitational constant. The expression  $\cos \alpha$  is modeling the influence of road inclination. [22, p.15]

$$F_r(v, p_t, \dots) = c_r(v, p_t, \dots) \cdot m_v \cdot g \cdot \cos(\alpha) \quad (3.3)$$

**Uphill Driving Force** The uphill driving force  $F_g$  results from gravity while driving a non-horizontal track. Equation 3.4 represents the dependency on the inclination angle.

$$F_g(\alpha) = m_v \cdot g \cdot \sin(\alpha) \quad (3.4)$$

#### Vehicle Operation Modes

Figure 3.2 shows the three main modes of vehicle operation:

- $F_t > 0$  *traction*, propulsion force is provided
- $F_t < 0$  *breaking*, the breaking- and/or the recuperating system is dissipating kinetic energy of the vehicle
- $F_t = 0$  *coasting*, the engine and the electric motor are disengaged. Here the decrease of kinetic energy is equal to the resistance losses. The function of coasting velocity  $v_c$  is derived in [22, p.20 et sqq.].

### 3 Methodology

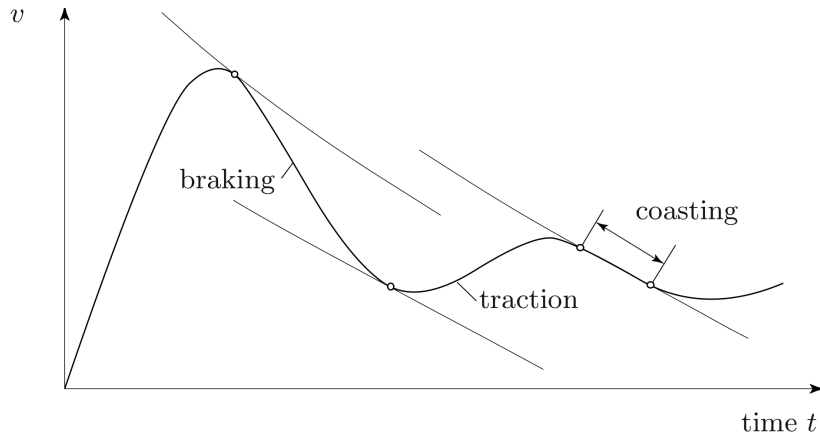


Figure 3.2: Different modes of vehicle operation. [22, p.20]

#### Propulsion Power

To make the vehicle follow a test cycle the required power needs to be transmitted by the drive train.

$$P_{prop}(t) = P_{f-axle}(t) + P_{r-axle}(t) \quad (3.5)$$

$$P_{trac}(t) = \begin{cases} P_{prop}(t) & , \quad \text{if } P_{prop}(t) > 0 \\ 0 & , \quad \text{else} \end{cases} \quad (3.6)$$

$$E_{trac}(t) = \int_{t_0=0}^t P_{trac}(t) dt \quad (3.7)$$

$$P_{break}(t) = \begin{cases} P_{prop}(t) & , \quad \text{if } P_{prop}(t) < 0 \\ 0 & , \quad \text{else} \end{cases} \quad (3.8)$$

$$E_{break}(t) = \int_{t_0=0}^t P_{break}(t) dt \quad (3.9)$$

## 3 Methodology

- Here the term  $P_{prop}(t)$  represents the total propulsion power of a vehicle over time. Its value is equal to the sum of transmitted power on front axle  $P_{f-axle}(t)$  and rear axle  $P_{r-axle}(t)$  like shown in equation 3.5.
- As described by the term 3.6 the traction power  $P_{trac}(t)$  is equal to propulsion power whenever it is positive during *traction* mode.
- As described by the term 3.8 the breaking power  $P_{break}(t)$  is equal to propulsion power whenever it is negative during *breaking* mode.

When  $P_{trac}(t)$  and  $P_{break}(t)$  gets integrated with respect to time the energy terms  $E_{trac}(t)$  and  $E_{break}(t)$  are resulting as shown in equation 3.7 and 3.9.

### 3.1.2 Subsystems

#### Subsystem IC Engine

Assuming a stable operation of the IC engine in a certain operating point the efficiency can be expressed by the equation 3.10.

- $\eta_e$  is the effective efficiency of combustion engine.
- $\omega_e$  is the angular speed of crankshaft.
- $T_e$  is the torque acting on crankshaft.
- $P_c$  is fuel supply's chemical flow of enthalpy.

$$\eta_e = \frac{\omega_e \cdot T_e}{P_c} \quad (3.10)$$

The fuel flow can be expressed by equation 3.11.  $H_l$  is the lower heating value of the fuel.

$$\dot{m}_f = \frac{P_c}{H_l} \quad (3.11)$$

### 3 Methodology

Engine maps are the most common way to specify ICE efficiency performance over a wide area of operation. One way of mapping ICE characteristics is the engine efficiency map. In figure 3.3 an efficiency map of a SI IC engine is shown. Here  $\eta_e$  is plotted over engine speed and engine torque. [22, p.47 et sqq.]

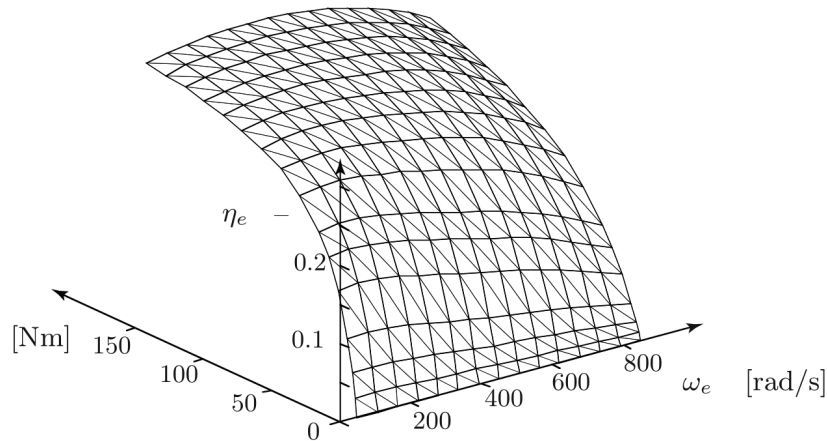


Figure 3.3: Efficiency consumption map of a SI IC engine. [22, p.37]

#### Subsystem Gearbox

The subsystem gearbox is transforming mechanical power. By a gear ratio the power supplied with a certain speed  $\omega_1$  and a certain torque  $T_1$  is converted to another speed  $\omega_2$  and another torque  $T_2$ . Without considering any losses the assumptions stated in equation 3.12 and 3.13 are valid.

$$\omega_1 = \varphi \cdot \omega_2 \quad (3.12)$$

$$T_2 = \varphi \cdot T_1 \quad (3.13)$$

$\varphi$  is representing the transmission ratio.

Of course, losses need to be taken into account for investigating the subsystem gearbox. Figure 3.4 illustrates an elementary model of the gearbox.

### 3 Methodology

An efficiency of the gearbox can be formulated by the approximation described in equation 3.14 (for a power flow from ICE to vehicle) and 3.15 (for a power flow from vehicle to ICE).

- $T_1$  and  $\omega_e$  are torque and speed at ICE side of gearbox.
- $\varphi$  and  $\eta_{gb}$  are the current transmission ratio and the gearbox efficiency.
- $T_2$  and  $\omega_w$  are torque and speed at vehicle side of gearbox.
- $P_{0,gb}(\omega_e)$  and  $P_{1,gb}(\omega_e)$  are representing the power needed for idling of the gearbox at the engine speed  $\omega_e$ .

[22, p.55]

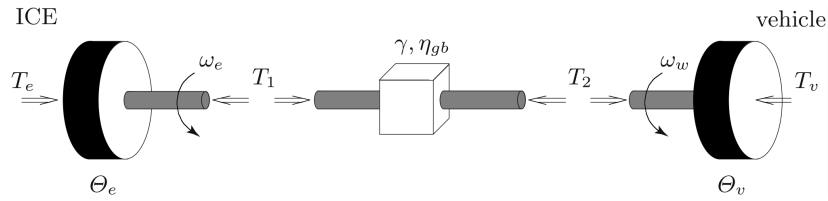


Figure 3.4: Gearbox model for definition of transmission efficiency. [22, p.54]

$$T_2 \cdot \omega_w = \eta_{gb} \cdot T_1 \cdot \omega_e - P_{0,gb}(\omega_e), \quad T_1 \cdot \omega_e > 0 \quad (3.14)$$

$$T_1 \cdot \omega_e = \eta_{gb} \cdot T_2 \cdot \omega_w - P_{1,gb}(\omega_e), \quad T_1 \cdot \omega_e < 0 \quad (3.15)$$

### 3.1.3 Power Flows in PHEV Drive Train

#### Different Operating Modes Parallel Hybrids

Since the emphasis of this work is on parallel hybrid concepts this technology is discussed in a little more detail. Figure 3.5 shows a simplified structure chart of an universal parallel hybrid configuration. At the torque converter (TC) the mechanical energy flow from electric propulsion and ICE propulsion are linked and balanced. As shown in equation 3.16 the value  $u$  describes the ratio between the energy flow from/to the electric machine and the total power at TC. When the electric machine is operating as a motor and is contributing propulsion torque the value of its

### 3 Methodology

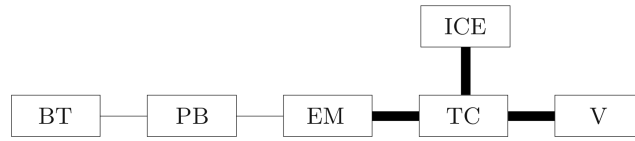


Figure 3.5: Simplified composition diagram of full parallel hybrid configuration. [22, p.72]  
 BT = Battery, PB = power link, EM = electric motor, ICE = combustion engine, TC = torque converter, V = axles and vehicle.

energy flow  $P_{EM}$  is positive and therefore the value of  $u$  is positive. When the electric machine is operating as a generator the value of  $u$  becomes negative. In case no power at all is transmitted by TC (for example while charging by ICE during vehicle's standstill) its value is  $-\infty$ .

$$u = \begin{cases} \frac{P_{EM}}{|P_{TC}|} & , \quad \text{if } P_{TC} \neq 0 \\ 1 & , \quad \text{else} \end{cases} \quad (3.16)$$

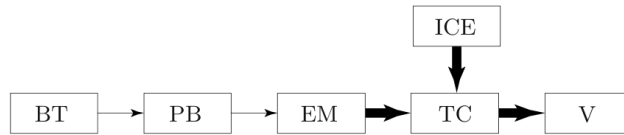
Figure 3.6 displays most relevant modes for parallel hybrid vehicle operation and the corresponding energy flows. [27]

#### Load-Point Shifting

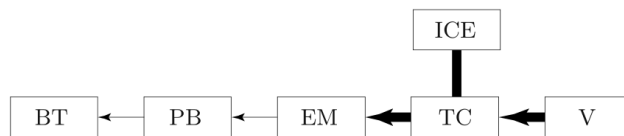
The Load-Point Shifting (LPS) program needs to respect engine specific factors like, for instance acoustic- and emission-limits. Here a general LPS-program is defined which can be applied to all the investigated combustion engines. With this program the level of LPS depends directly on the State of Charge (SOC). Figure 3.7 describes a typical heuristic energy-management for parallel hybrid vehicles. The torque ratio is displayed as a function of the desired torque and the vehicle speed. It can be seen that the areas of positive LPS are increasing with the decrease of SOC. Hence, it can be derived that the potential for battery recharging by LPS varies from IC engine to IC engine. Of course factors like acoustic- and emission limits are influencing the operating strategy as well. Nevertheless, for simplicity reasons, here these influences are just discussed secondarily.

### 3 Methodology

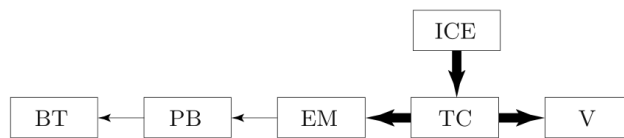
(a) power assist,  $0 < u < 1$



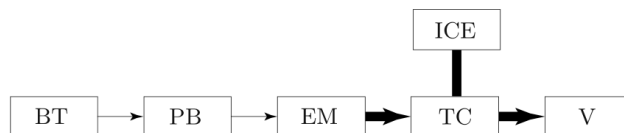
(b) regenerative braking,  $u = 1$



(c) battery recharging,  $u < 0$



(d) ZEV,  $u = 1$



(e) conventional vehicle,  $u = 0$

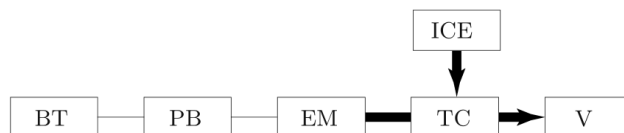


Figure 3.6: Power flow for PHEV operating modes. [22, p.76]  
ZEV = zero emission vehicle

### 3 Methodology

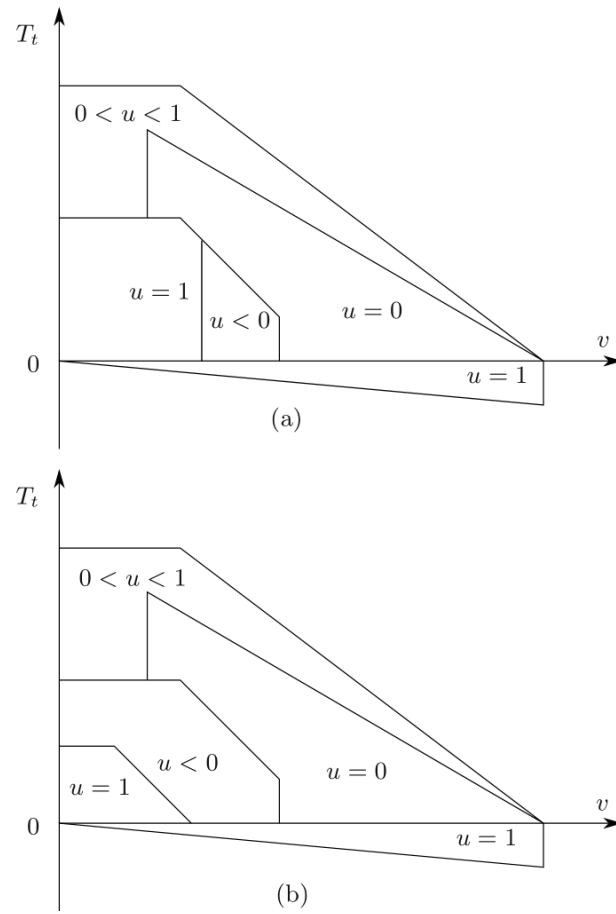


Figure 3.7: Energy management of parallel hybrid drive train. [22, p.248]  
(a) for high SOC, (b) for lower SOC

### 3 Methodology

#### Acceleration-Velocity Characteristic

For the analysis of this work electric operating strategies (eOS) are mainly defined by an acceleration-velocity (AV) characteristic. Figure 3.8 explains the general functionality of IC engine start-/stop system. The event of an ICE start happens whenever driving situation is exceeding the ICE-start AV-characteristic (continuous line) towards a combination of greater vehicle speeds and greater vehicle accelerations. An ICE stop is triggered whenever driving situation falls below the ICE-stop AV-characteristic(dashed line). [29]

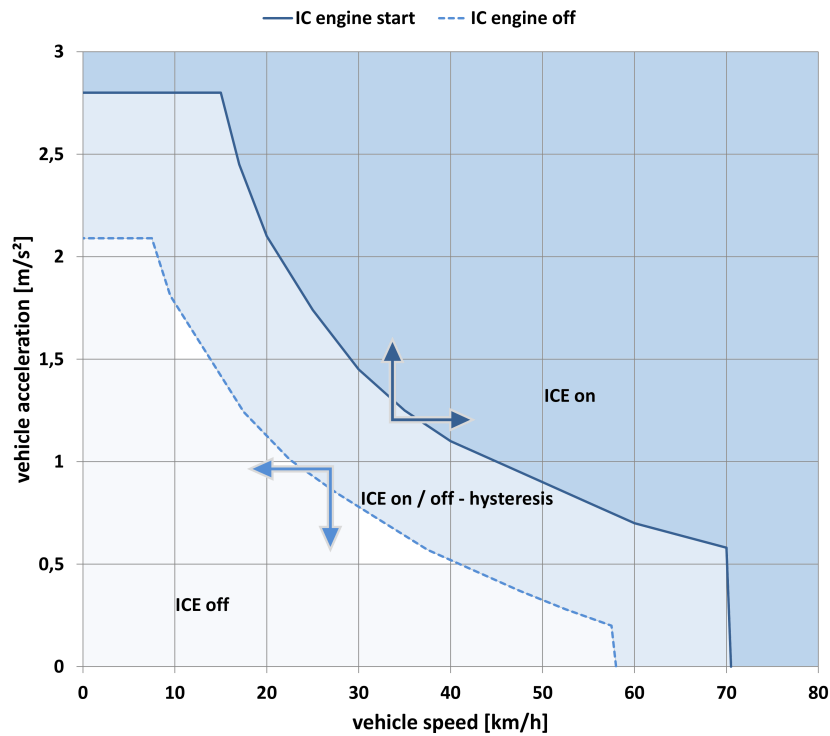


Figure 3.8: Functionality of IC engine on-/off characteristic.

## 3 Methodology

### Charge Sustaining Criterion

In general the aim for CS testing is to evaluate the hybrid system without consuming energy from battery. Therefore the propulsion energy taken out of battery needs to be compensated by conducting recuperation and load-point-shifting (see section 3.1.3). In order to allow standardized testing with different vehicle models the CS-criterion has been defined:

A test cycle is conducted with respect to the CS criterion whenever the SOC difference between cycle start and cycle end is smaller than a defined tolerance. The CS criterion which has been defined for this work is

$$|SOC_{end}| - |SOC_{start}| \leq 0,05 \text{ kWh}. \quad (3.17)$$

Here, the value of 0,05 kWh has been found adequate for analysis. It defines a sufficient level of accuracy and enables a practicable number of iteration cycles in simulation to reach CS criterion.

### 3.2 Vehicle Definition

Due to the objectives stated in chapter 1.2 a variety of IC engines needs to be investigated to enable a sound statement. Therefore a vehicle is specified which allows the usage of different IC engines with a wide range of propulsion power. A D-segment model has been found as a representative vehicle platform [17]. First, the D-segment stands for models of high sales volume and thus, high relevance [11]. Second, this segment can be adequately powered by all IC engines for this analysis (introduced in section 3.2.3). In the following the conventional and the plug-in hybrid vehicle are defined as testing platforms.

### 3.2.1 Conventional Vehicle

Specifications of conventional D-segment model are stated in table 3.1. Here the value of rolling resistance is determined at a vehicle speed of  $100 \text{ km/h}$ .

Table 3.1: Technical specification of conventional vehicle.

Unloaded mass	$m$	=	1410 kg
Drag coefficient	$c_x$	=	0.25
Frontal area	$A_{front}$	=	$2.2 \text{ m}^2$
Rolling-resistance coefficient	$RRC$	=	0.0084

Figure 3.9 shows the topology of this vehicle platform. Here the IC engine is placed alongside in the front. The propulsion power is transmitted through the torque converter into the gearbox. At the output end of gearbox the power is transferred by cardan shaft to the rear-axle differential. Inside rear-axle differential another transmission ratio is realized before the power gets passed on to the wheels.

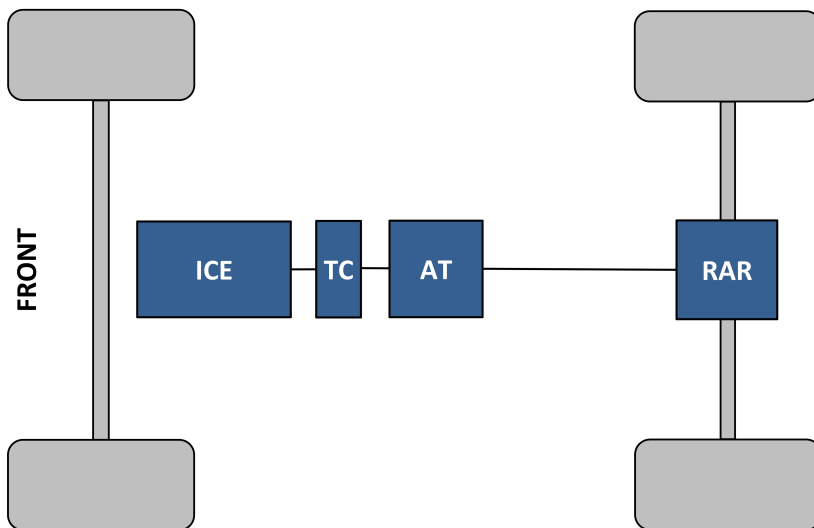


Figure 3.9: Topology of conventional vehicle.  
Rear-wheel drive with IC engine placed alongside in front.

### 3.2.2 Plug-in Hybrid Electric Vehicle

Due to the on board electrification technology, PHEV vehicles have significantly different properties. From total vehicle perspective the most relevant differences are the extra-mass, which is mainly caused by the battery, and an increased drag coefficient, which is resulting of greater necessary cooling area. In terms of driving experience, extra weight gets compensated by the additional propulsion power from the electric machine. The specifications for the PHEV D-segment model are stated in table 3.2.

Table 3.2: Technical specification of plug-in hybrid vehicle.

Unloaded mass	$m$	=	1660 kg
Drag coefficient	$c_x$	=	0.27
Frontal area	$A_{front}$	=	2.2 m <sup>2</sup>
Rolling-resistance coefficient	$RRC$	=	0.0084

Figure 3.10 shows the drive train topology of investigated PHEV vehicle. As can be seen a P2 parallel hybrid arrangement is matter of investigation [23]. The IC engine is placed alongside in the front of vehicle. A clutch placed in between IC engine and the electric motor/generator allows electric drive only. Regarding the packaging issue the electric motor/generator is integrated inside the gearbox housing. At the output end of gearbox the power is transferred by cardan shaft to the rear-axle differential. The transmission ratio of the rear-axis differential is specifically adjusted for PHEV drive train. From the rear-axis differential the power gets passed on to the wheels. [6]

### 3.2.3 Subsystems

#### IC Engines

Since each motorization interacts differently with the vehicle different ranges of operation are resulting. In order to find a common basis for

### 3 Methodology

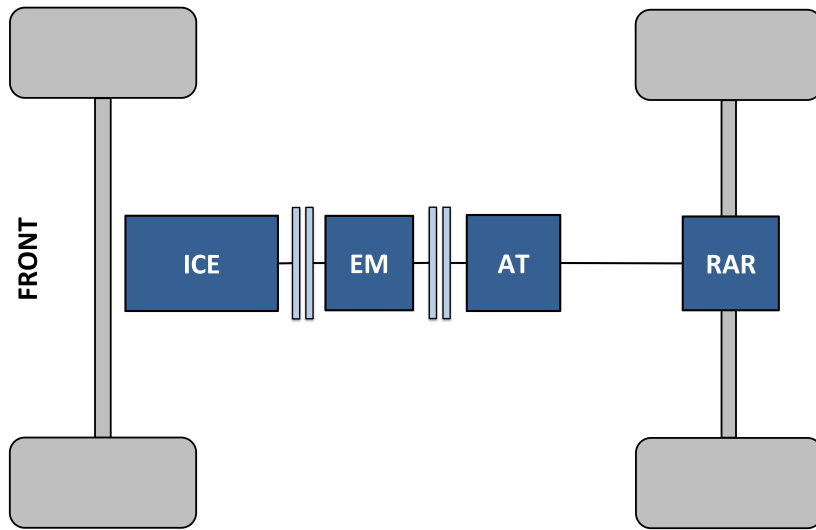


Figure 3.10: Topology of PHEV vehicle.  
Rear-wheel drive with IC engine placed alongside in front.

evaluation, IC engines with similar characteristics are summarized to classes specified by engine type and power level. The engine type is differentiating between gasoline engines (spark ignited (SI)) and diesel engines (compression ignited (CI)). Here two power levels are introduced, the 100 kW level and the 140 kW level. Investigation is conducted for SI IC engines in both power classes and for CI IC engines the 140 kW level is selected.

For conducting reference simulations each class needs to be represented by one IC engine. In table 3.3 three IC engines are listed and specified which have been found most appropriate.

Table 3.3: Reference IC engines for simulation. [13][15][14]

power class	ICE type	displacement	torque
100 kW	B38A15	1,499 cm <sup>3</sup>	220 Nm at 1250 – 4300 rpm
140 kW	B48A20	1,998 cm <sup>3</sup>	280 Nm at 1250 rpm
140 kW	B47D20	1,998 cm <sup>3</sup>	400 Nm at 1750 – 2500 rpm

## 3 Methodology

### Gearbox

Transmission spreading and gear ratios are highly influential for the range of operation of IC engine. For this analysis the gearbox specified in table 3.4 is used. For conventional- as well as for PHEV vehicle the same gearbox data is used.

Table 3.4: Reference gearbox for simulation. [39]

Transmission type	8HP45
Input torque	max. 450 Nm
Gear / standard ratios	
1	4,714
2	3,143
3	2,106
4	1,667
5	1,285
6	1,000
7	0,839
8	0,667
Transmission spreading	7,071

### 3.3 Use Case

In this section the use case for vehicle testing will be defined. First the relevant velocity profiles and propulsion power evaluations are discussed. Second vehicle specific settings are introduced. Third the testing procedure is explained.

#### 3.3.1 Test Cycles

Two test cycles are used for conducting the analysis of this work, the New European Driving Cycle (NEDC) and the Worldwide harmonized

### 3 Methodology

Light vehicle Test Cycle (WLTC). It has to be mentioned that these test cycles are normally embedded in testing procedures. Here for simplicity reasons the procedures are spared out and just the velocity profiles are taken into account.

#### New European Driving Cycle

The test cycle NEDC is designed to evaluate fuel consumption and emissions of European passenger cars. As can be seen in figure 3.11 four urban driving cycles and one extra-urban driving cycle are building the overall velocity profile. Some relevant key facts are summarized in table 3.5.

Table 3.5: Specifications of NEDC test cycle. [33]

Total distance	=	11023 <i>m</i>
Duration	=	1180 <i>s</i>
Maximum speed	=	120 <i>km/h</i>
Average speed	=	33,6 <i>km/h</i>
Number of stops	=	13

#### Worldwide Harmonized Light Vehicle Test Cycle

The driving cycle WLTC is representing the velocity profile for a globally harmonized testing standard. Figure 3.12 displays this driving cycle which consists out of four parts. Their durations are stated in 3.6

Table 3.6: Duration of WLTC test cycle parts.

Low	=	589 <i>s</i>
Medium	=	433 <i>s</i>
High	=	455 <i>s</i>
Extra High	=	323 <i>s</i>

Some relevant key facts are summarized in table 3.7.

### 3 Methodology

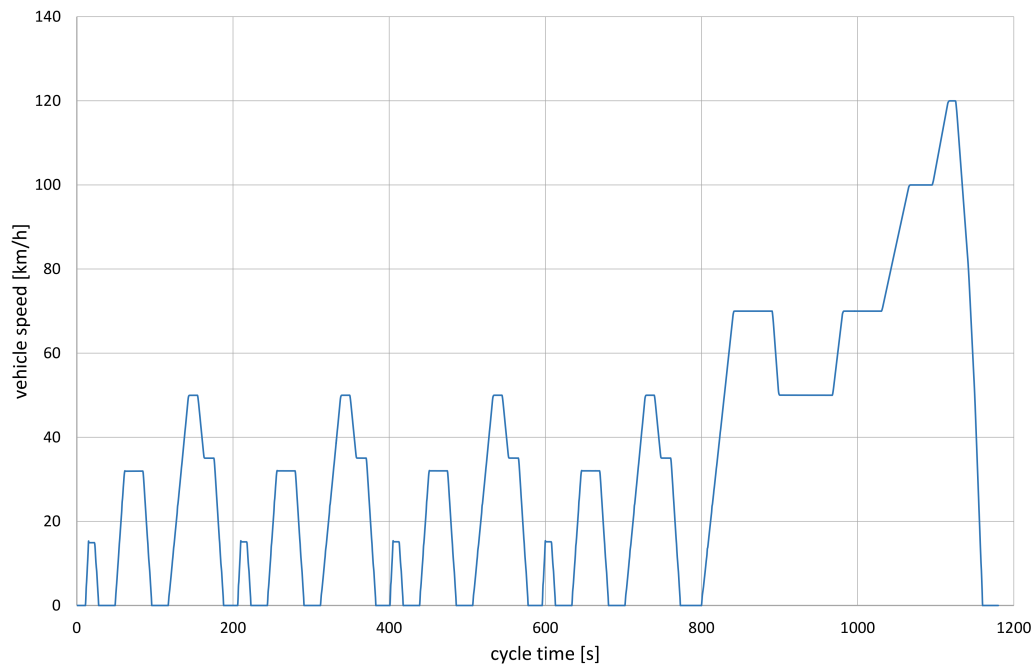


Figure 3.11: Velocity Profile of NEDC.

#### 3.3.2 Procedure of Evaluation

It is assumed that the system is tested in warm-state. Therefore effects of vehicle warm-up are not taken into account. The most important of these effects are the extra consumption for catalyst heating and the increased friction during IC engine warm-up. In consequence of this warm-state testing one test cycle is sufficient for evaluation. Hence, from the framework of NEDC and WLTP testing only the driving cycles themselves are

Table 3.7: Specifications of WLTC testcycle. [35] [34]

Total distance	=	23262 m
Duration	=	1800 s
Maximum speed	=	131,3 km/h
Average speed	=	46,5 km/h
Number of stops	=	8

### 3 Methodology

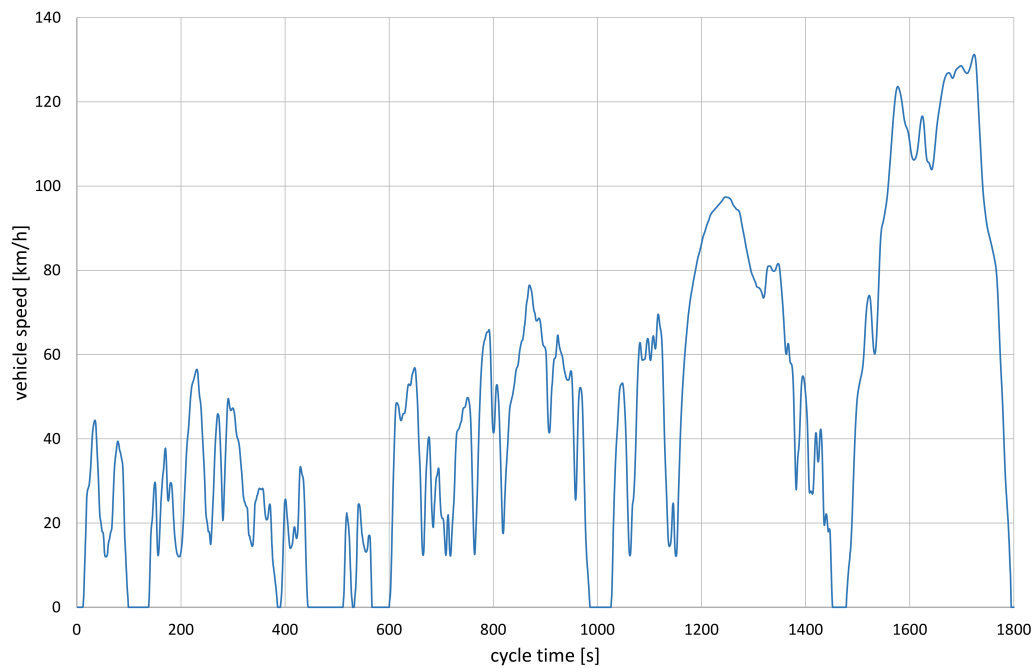


Figure 3.12: Velocity Profile of WLTC.

relevant for this analysis.

#### Conventional Vehicle

With the conventional vehicle as specified in section 3.2.1 one test run in a driving cycle of NEDC or WLTC is conducted. As mentioned, the vehicle is considered, having reached warm-state prior to testing. Ergo catalytic heating and engine warm-up are no subjects of investigation. For transmission testing the same boundary conditions are applied.

#### Plug-in Hybrid Electric Vehicle

The overall vehicle specifications for the PHEV have been defined in section 3.2.2. For consumption considerations the electric range and the energy usage during pure electric drive is not of interest. Therefore here

## 3 Methodology

a test run in the mode " State of Charge (SOC) minimum" is conducted. This mode is also called Charge-Sustaining (CS) and is introduced in section 3.1.3. For IC engine use no extra consumption for catalytic heating and engine warm-up is considered.

Since the gearbox in the PHEV vehicle (see section 3.2.2) is also transmitting energy during recuperation phases, it is essential that the driving mode allows a maximum of recuperation. This is guaranteed when vehicle is tested in SOC-min mode. Thus, the described testing conditions for determining ICE consumption are also perfectly applicable for gearbox evaluation.

### 3.3.3 Operating Strategy

In this section the most relevant factors for vehicle operation and their consequence on IC engine- and gearbox use are discussed. Due to the combination of combustion and electric propulsion PHEV's drive train operation is by far more complex than the conventional one. Therefore the emphasis of this section is clearly put on the introduction and definition of the PHEV operating strategy.

#### Conventional Vehicle

The conventional vehicle is tested as a reference to the PHEV vehicle. The testing procedure is introduced in section 3.3.2. During the whole test run an auto start-/stop function is active. The characteristic of this function causes an IC engine stop as soon as the vehicle decelerates to standstill. During deceleration phases without propulsion power demand the IC engine remains operating. Another influence is given by the gear shifting program. Since the selected gears are directly influencing the operating range of the IC engine this detail is highly relevant. For comparability reasons it is crucial to define one shifting program for all test runs. Here this program is defined by the default-mode settings after vehicle start.

In the following, IC engines characteristic of operation during different test cycles is described.

### 3 Methodology

**Operation in NEDC** Figure 3.13 shows the distribution of loadpoints of a 140 kW SI IC engine which is operating in the conventional vehicle while test-running a NEDC. The timestep of spotted loadpoints is 2 seconds. Furthermore the consumption weighted average (cons av) is indicated by the fattened spot. It can be observed that engine range of operation is distributed widely in low power area.

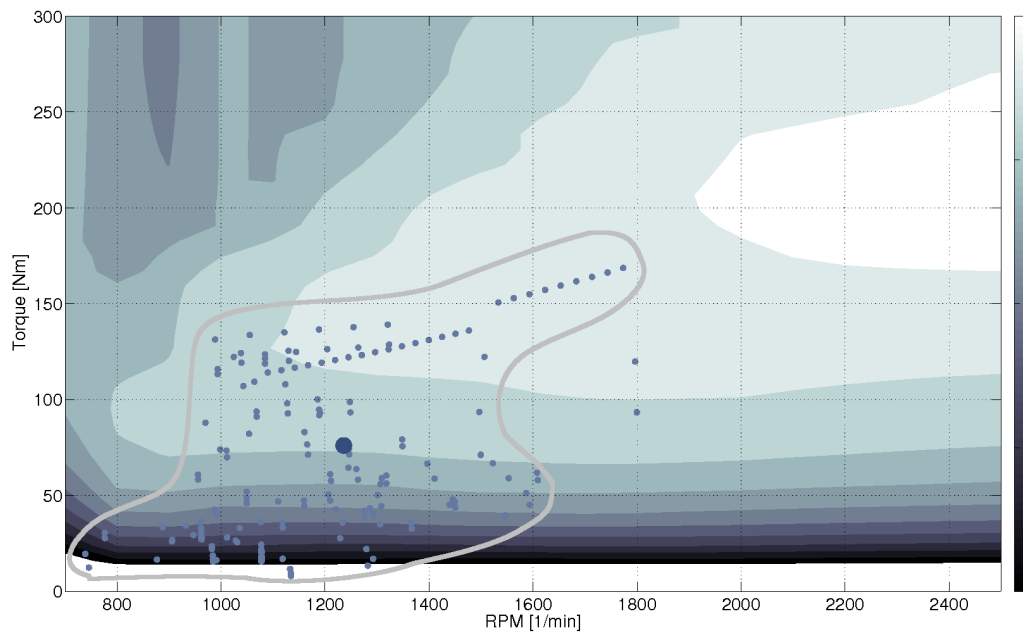


Figure 3.13: Distribution of load points / 140kW SI IC engine operating in conventional vehicle in NEDC.

**Operation in WLTC** Figure 3.14 shows the distribution of loadpoints of a 140 kW SI IC engine while test-running a WLTC. Also here the timestep of spotted loadpoints is 2 seconds. The consumption weighted average is indicated by the fattened spot. Generally it can be stated that IC engines range of operation is distributed in areas of greater loads than during NEDC test-run. But still the range of operation is spread widely.

### 3 Methodology

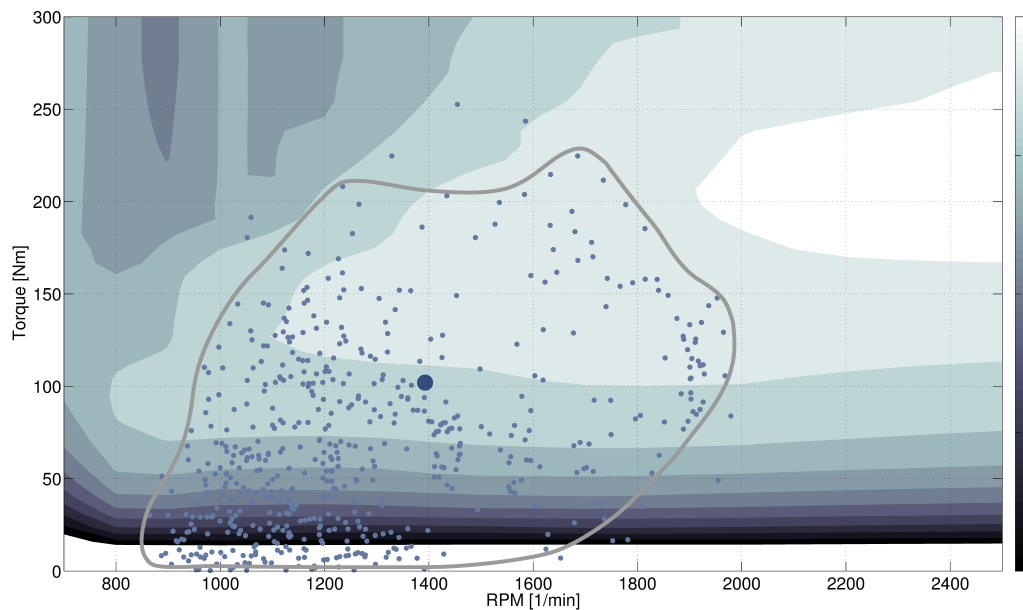


Figure 3.14: Distribution of load points / 140kW SI IC engine operating in conventional vehicle in WLTC.

#### Plug-in Hybrid Vehicle

For plug-in hybrids significantly more parameters have to be stated in order to realize comparable circumstances and a defined operating strategy. Although the gear shifting program during pure electric drive usually has different characteristics than during ICE driven periods, here one elementary constraint is that the PHEV gear shifting program is equal to conventional vehicles program, regardless whether vehicle is powered by electric motor or IC engine.

For hybrid drive train, another crucial condition is the IC engine on-/off characteristic during a test cycle. This characteristic is defined by a systematic, depending on vehicles acceleration and velocity (av-characteristic) as described in section 3.1.3. According to this systematic IC engines operation is directly depending on the test cycle, since it is defining vehicles acceleration and velocity over time. The operating strategies, which are described in the following, were created with respect to the test cycle and the overall vehicle specification as the two greatest factors of influence.

### 3 Methodology

In the following the different electric Operating Strategies (eOS) for the PHEV vehicle are introduced. Here the characteristic of operation is indicated by the IC engine on-/off pattern as well as by the ICE operating range.

**NEDC Efficient Strategy / eOS 1** Figure 3.15 is representing an IC engine on-/off pattern, indicated by blue and white areas beneath the velocity profile. Here the filled out areas mark the IC engine operating periods. Furthermore this chart is indicating the state of charge (SOC) over time by the dashed line on the second scale. Moreover the periods with active load-point shifting are expressed by the increase of SOC. The generator use of the electric machine and therefore battery charging by LPS can be read from the positive slope of SOC during periods of ICE operation.

For finding a very efficient operating strategy an optimization algorithm was used. It has been found that for greater power demands, during acceleration and high speed periods, the PHEV drive train is more efficient, applying IC engine propulsion rather than electric propulsion. Therefore the efficient AV-characteristic is triggering an ICE start whenever greater propulsion power is demanded. The ICE on-/off periods shown in figure 3.15 result directly out of this efficient operating strategy. It can be seen that the ICE on-/off pattern is rather continuous during whole test cycle and an ICE-start is triggered whenever propulsion power is demanded. The focus for the application of this strategy is clearly to minimize fuel consumption. The driving experience is not of any relevance. Figure 3.15 shows the distribution of loadpoints of the 140 kW SI IC engine during a NEDC eOS 1 test-run. The timestep of the spotted loadpoints is 2 seconds. The consumption weighted average is indicated by the fattened spot. Compared to the conventional vehicle, here the IC engines operating range is clearly more isolated in an area of greater torques and greater speeds. Most of the low power operating points are driven by the electric machine.

**NEDC Drain & Recharge Strategy / eOS 2** A system which is initiating an ICE start whenever minor acceleration is demanded is expected to

### 3 Methodology

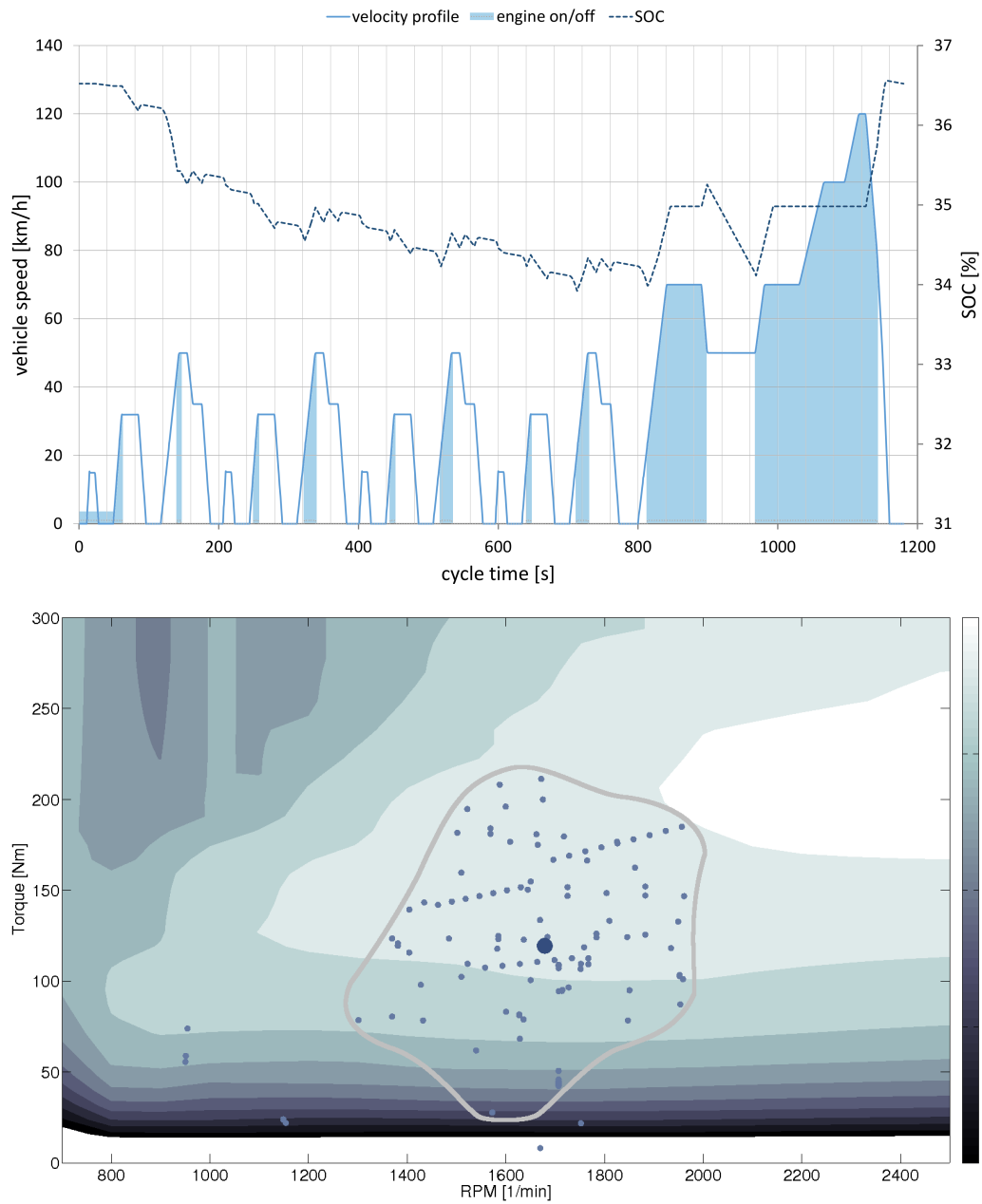


Figure 3.15: Top: SOC and ICE on-/off periods with eOS 1 in NEDC.  
Bottom: Distribution of load points / 140kW SI IC engine with eOS 1 in NEDC.

### 3 Methodology

cause negative driving experience. For eOS 2 it is assumed that pure electric drive during the urban part of driving cycle would be appreciated by the customer. During pure e-drive periods all propulsion energy is taken from the battery. Therefore, in order to compensate the consumed energy, the PHEV system is conducting heavy load-point shifting while the IC engine is operating during extra-urban part of cycle. Figure 3.16 points out the ICE on-/off periods as well as the SOC development over cycle-time. Furthermore the SOC developing is indicating heavy LPS for recharge during the ICE operating periods. In figure 3.16 the range of operation of the 140 kW SI IC engine during a NEDC eOS 2 test-run is shown. The timestep of the spotted loadpoints is 2 seconds. The consumption weighted average is indicated by the fattened spot. By applying this strategy it can be observed that IC engines operating range is isolated even more than by applying eOS 1. Compared to eOS 1, here the IC engine is operated in greater torques where the engine speed stays constant. This can be explained since the gear shifting strategy is not directly affected by the electric operating strategy as long as IC engine is not reaching its full load limit.

**WLTC Efficient Characteristic / eOS 3** For vehicle analysis in WLTC one efficient operating strategy has been selected. Therefore IC engine propulsion is used for greater demanded power. The electric drive is just contributing during periods of little demanded power. The resulting ICE on-/off periods as well as the developing of SOC are illustrated in figure ???. The pattern of IC engine operation is rather continuous. For this operating strategy driveability issues have not been taken into account. In figure ??? the range of operation of the 140 kW SI IC engine during a WLTC eOS 3 test-run is shown. The timestep of spotted loadpoints is 2 seconds. The consumption weighted average is indicated by the fattened spot. Compared to the conventionally driven vehicle, also in WLTC it can be seen that operating points develop towards greater torques and greater speeds. Furthermore the range is more isolated.

### 3 Methodology

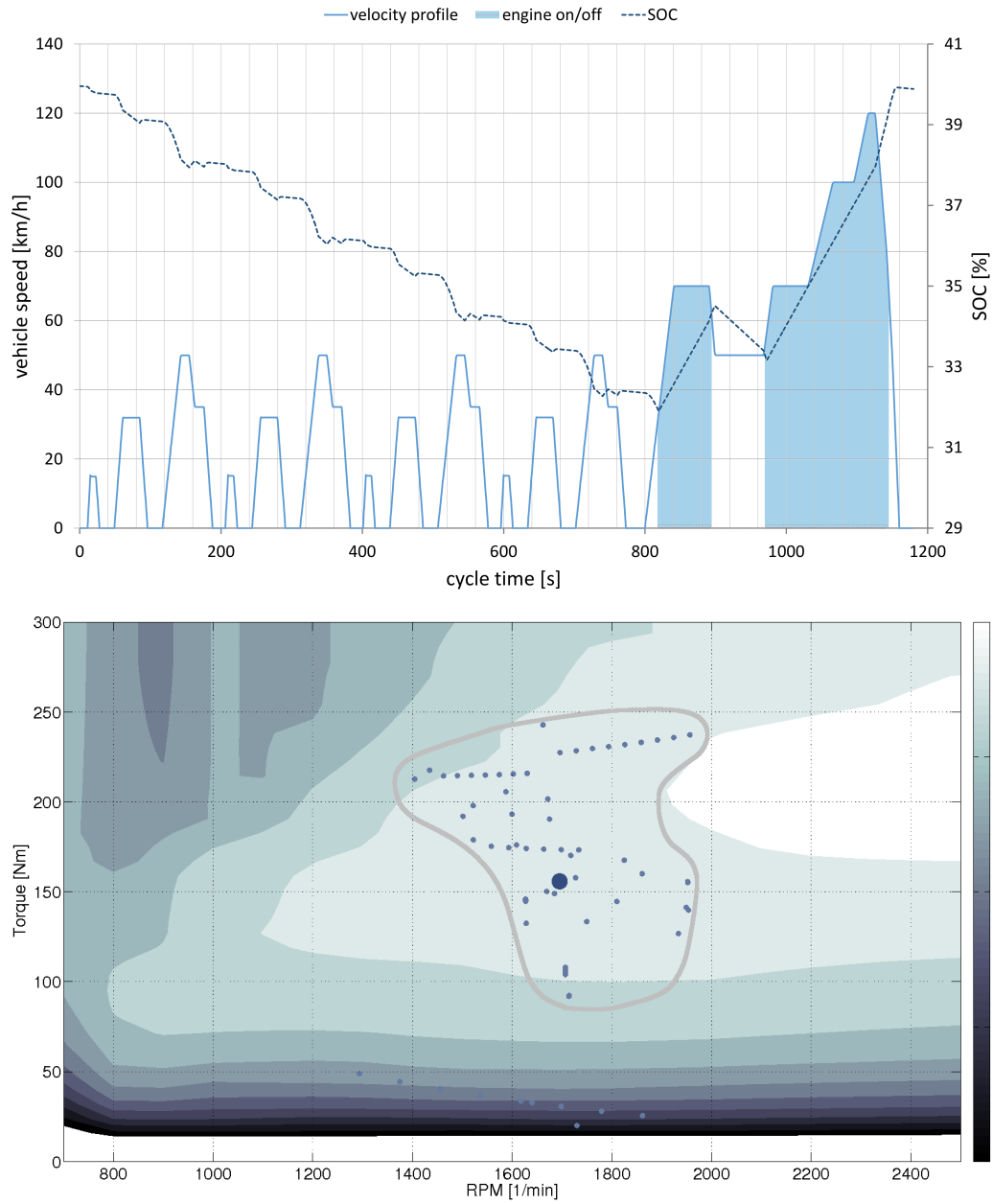


Figure 3.16: Top: SOC and ICE on-/off periods with eOS 2 in NEDC.  
Bottom: Distribution of load points / 140kW SI IC engine with eOS 2 in NEDC.

### 3 Methodology

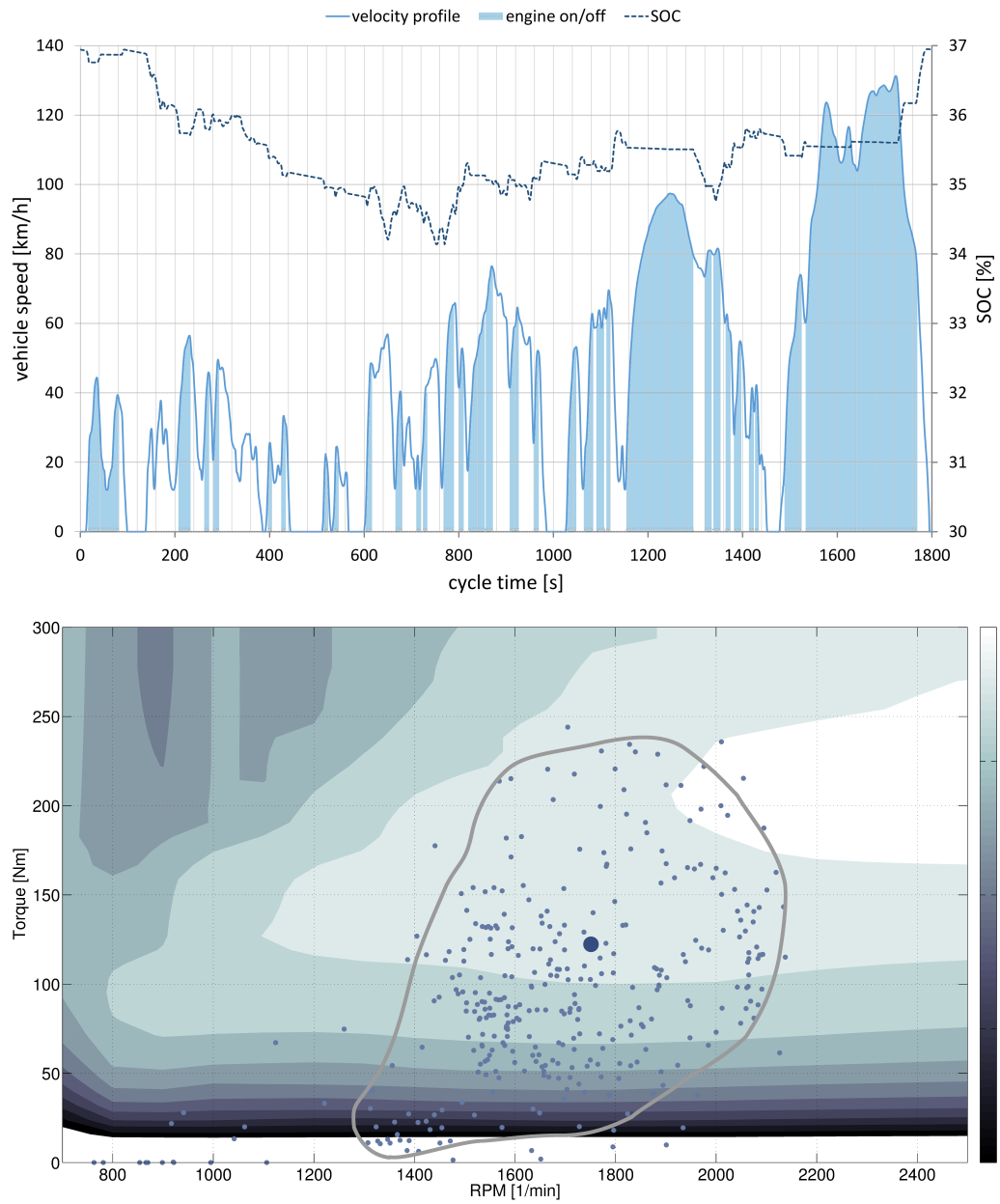


Figure 3.17: Top: SOC and ICE on-/off periods with eOS 3 in WLTC.  
Bottom: Distribution of load points / 140kW SI IC engine with eOS 3 in WLTC.

### 3.4 Simulation Model

Many investigations of this work are based on an longitudinal vehicle model implemented in the Dymola-Modelica environment. Modelica is an object oriented programming language for heterogeneous, large and complex models of physical systems. The model is described by differential, algebraic and discrete equations. [2, p.30 et sqq.]

#### 3.4.1 Longitudinal Vehicle Model

Figure 3.18 displays the composition diagram of longitudinal vehicle model. As the can be seen, a forward simulation algorithm is used [3]. Therefore a driver-controller is deriving the desire for acceleration or deceleration for each time-step from the developing of test cycle's velocity profile. The most relevant output of this controller is the accelerator-pedal position. As a consequence the simulation model computes this input with respect to vehicle specifications and the selected transmission ratio and passes on a signal for the desired effective engine torque. For the subsystem IC engine the desired effective engine torque as well as the current engine speed are the most important input signals. For the subsystem gearbox the current accelerator-pedal as well as the current engine speed are most relevant. In the subsequent sections these simulation models will be described in more detail. [3]

#### 3.4.2 IC Engine Model

In simulation environments there are various ways of modeling the characteristic of IC engines. In order to calculate fuel consumption the quasi-static calculation is a reliable approach. For this method the effective engine torque as well as the engine speed are determined for each time-step. Next these two signals are assumed to be constant during the short period of time of each calculation time-step. Hence, a static consumption map can be used to determine fuel consumption. For consumption calculation there are more simple ways to specify IC engine's efficiency than

### 3 Methodology

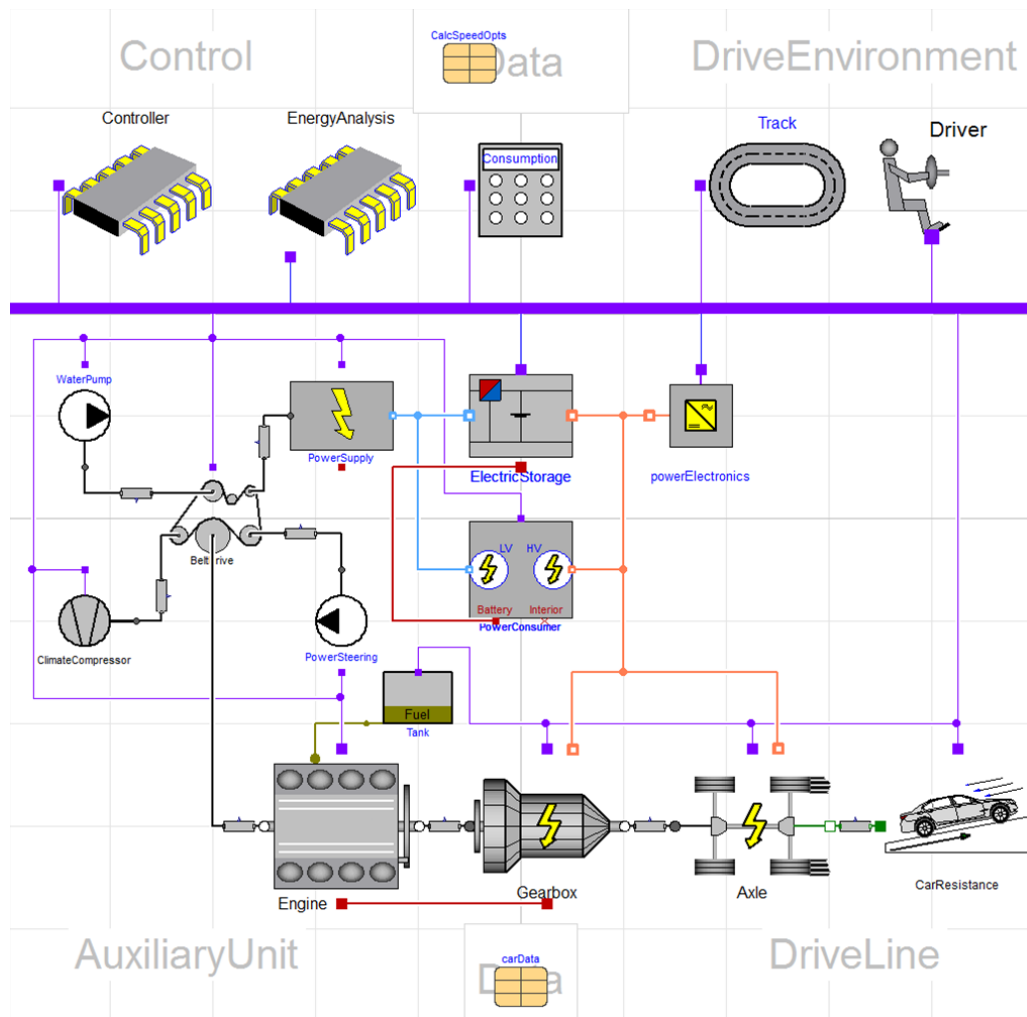


Figure 3.18: Simulation composition diagram of longitudinal vehicle model.

### 3 Methodology

the engine efficiency map shown in figure 3.3. By basic thermodynamic expressions this map can be converted to various different forms. One very useful form for simulation is the consumption map as represented in figure 3.19. It expresses the fuel use volume per operating time. Here the unit of consumption values is liters fuel per hour [ $l/h$ ]. These values are plotted with respect to engine speed [ $rad/s$ ] and engine torque [ $Nm$ ].

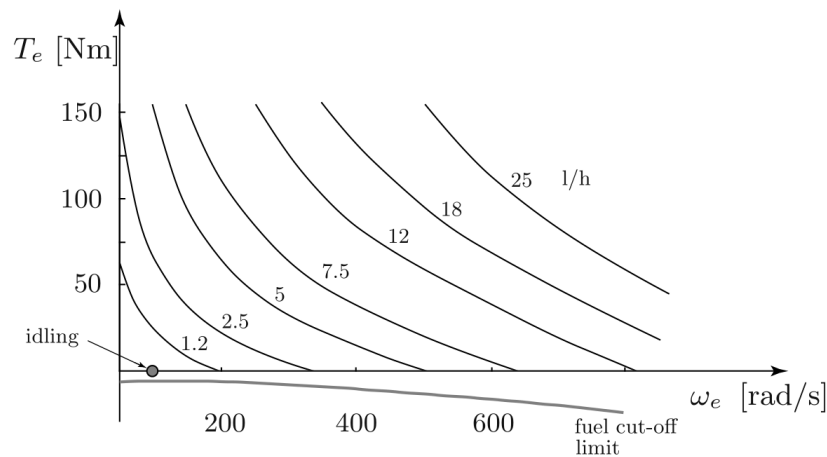


Figure 3.19: Fuel flow consumption map of a SI IC engine. [22, p.39]

In simulation this consumption map is implemented in form of a two dimensional look-up table. As already mentioned, here the most relevant input variables are *engine speed* and *effective engine torque*. The value for fuel consumption per time can be read with respect to these input variables. The output signal is of the unit  $l/h$  and therefore needs to be multiplied by the duration of the time-step in hours. By integration over operating time the total fuel consumption of the IC engine can be determined.

As has been shown in section 3.3.3, a PHEV can be operated in different modes by applying different electric operating strategies. Therefore the operating strategy is defining the systematic of interaction of all the subsystems. For the IC engine a change in strategy also signifies a change of the specific use pattern. One way of describing this use pattern is to mark the range of operation by plotting the operating point of each

## 3 Methodology

time-step within the consumption map. Hence, a defined use case of an IC engine can be derived from range of operation during a test cycle. In chapter 4 the characteristic of various IC engines use cases will be discussed and compared.

### 3.4.3 Gearbox Model

Here two elementary functions of the gearbox model are briefly discussed. First, the functionality of gear selection. Second, the model of friction losses.

#### Gear selection

The gear selection characteristic is defined by the gear shifting strategy diagram. The input variables for this diagram are engine speed and acceleration-pedal position (APP). The data sets of these shifting diagrams are discussed in more detail in section 4.2.

#### Friction losses

The most important influential factors for friction losses in gearbox are the selected gear, input speed and torque and the temperature. Within the model gearbox losses are determined by two-dimensional characteristics modeled in a look-up table. Input characters for these tables are input speed and torque. As an output the current value for friction torque is received. To take the specific characteristic of the selected gear into account the look-up table is implemented gear wise. Hence, for each gear a separate look-up table is used, for determining friction torque. For the temperature effect the same approach is used, whereas step-size is 10 K within the relevant temperature range.

### 3.5 Matlab Tool for Consumption Calculation

The longitudinal vehicle simulation environment, introduced in section 3.4, is perfectly valid to process a specified vehicle set up, with all corresponding subsystems, in chosen use case. In this simulation environment the IC engine characteristic needs to be introduced by a so called member-files. These files contain all necessary information about the IC engine such as the number of cylinders, the engine displacement, the consumption map, emission maps, full load characteristic and many more. At simulation start Dymola-/Modelica-environment integrates this information and initiates the simulation process. During simulation process a lot of interactions between subsystems and the vehicle are calculated and the operating strategy of the IC-engine gets influenced. Thus, these interactions are also influencing the operation of subsystems. Figure 3.20 charts exemplary interactions between IC engine characteristics and influencing factors for ICE operation.

However, for overall vehicle considerations simulation is very powerful. For specific investigation of subsystem performance such as the efficiency of an IC engine problems are arising:

1. Because of interactions, it is difficult to implement clear boundary conditions for comparison investigations.
2. For each test of a specifically described IC engine, a lot of peripheral data needs to be processed on overall vehicle level. Therefore a lot of simulation time is consumed for irrelevant processing.
3. Due to the complexity of the longitudinal vehicle simulation model it is difficult to make specific changes without causing unwanted interactions with the rest of the model.

These are some of the reasons why a simplified calculation environment needed to be introduced. In the subsequent section a developed Matlab calculation will be explained in more detail.

### 3 Methodology

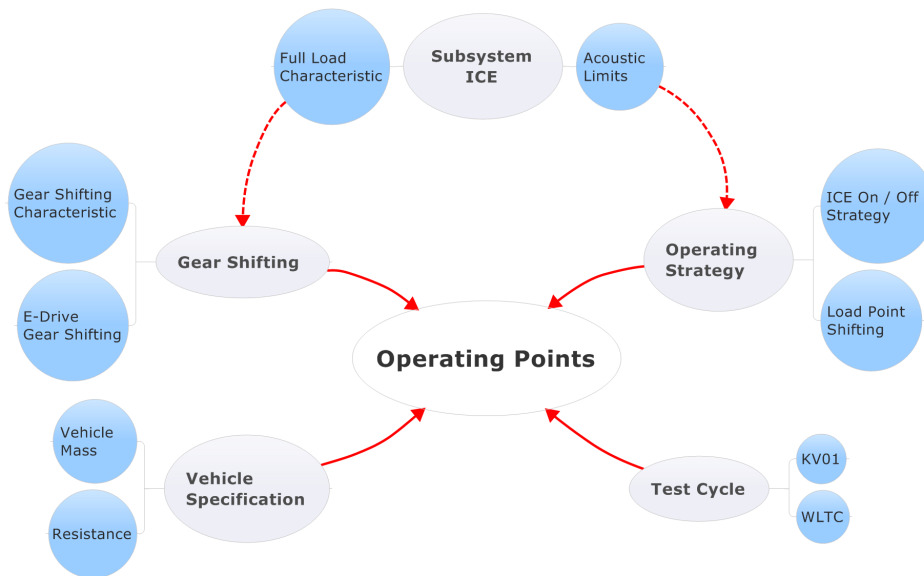


Figure 3.20: Exemplary interactions between ICE characteristics and external influential factors for ICE operation.

#### 3.5.1 Systematic of Calculation

As mentioned, a basic motivation for introducing a simplified calculation method, is the necessity to keep the boundary conditions the same for analyzing IC engine operation. Especially for a valid comparison of different engine concepts, this is crucial.

#### Set of ICE Operating Points as Basis of Valuation

Looking at the IC engine as an isolated subsystem, it is the developing of engine torque and engine speed over time which describes the condition of operation. In every time-step these two signals are defining one

### 3 Methodology

operating point in an engine map. By plotting the operating point of every time-step while vehicle is running a test cycle, a set of operating points will be defined. Since this set of operating points is the result of a monitoring process, it can be seen as the description of ICE operation during test cycle. In section 3.3.3, various sets of operating points within the conventional and the PHEV vehicle in different test cycles are shown. Here each operating point stands for two seconds of operation. Hence, the complete set of operating points monitored during a test cycle run is appropriate to build the basis of valuation. For describing quantities of operation, average values are useful. The average is only build over periods of IC operation.

**Time-weighted average** For evaluating the time-weighted average, the duration of each time-step is taken as a weighting factor. Equation 3.18 describes how the time-weighted average of engine speed  $\bar{S}_{time}$  and effective engine torque  $\bar{T}_{time}$  can be determined.  $S$  is an output value of engine speed from simulation.  $T$  is an output value of effective engine torque from simulation.  $t_{step}$  is the duration of the corresponding time-step.  $t_{tot}$  is the total duration of test-period. The index  $i$  stands for the number of the output value.  $N$  is the total number of output values in test period.

$$\begin{aligned}\bar{S}_{time} &= \frac{1}{t_{tot}} \sum_{i=1}^N S_i \cdot t_{step\ i} \\ \bar{T}_{time} &= \frac{1}{t_{tot}} \sum_{i=1}^N T_i \cdot t_{step\ i}\end{aligned}\tag{3.18}$$

**Consumption-weighted average** For evaluating the consumption-weighted average, the consumption value of each time-step  $c$  is taken as a weighting factor. Since the consumption depends on engine speed and effective engine torque, consumption map needs to be read for each time-step. A consumption value in fuel volume per time is received. Equation 3.19 describes how the consumption-weighted average of engine speed  $\bar{S}_{cons}$  and effective engine torque  $\bar{T}_{cons}$  can be determined.

### 3 Methodology

$$\begin{aligned}\bar{S}_{cons} &= \frac{\sum_{i=1}^N S_i \cdot c_i \cdot t_{step\ i}}{\sum_{i=1}^N c_i} \\ \bar{T}_{cons} &= \frac{\sum_{i=1}^N T_i \cdot c_i \cdot t_{step\ i}}{\sum_{i=1}^N c_i}\end{aligned}\tag{3.19}$$

#### Consumption Calculation

By applying the quasi-static fuel calculation approach, introduced in section 3.4.2, the specific consumption of operation (in liters per hour) in each operating point can be determined by using an engine consumption map as shown in figure 3.19. For receiving the absolute fuel consumption of each point, the specific value needs to be multiplied by the duration of each time-step. By doing so for every point of the whole set and by building the sum of all point-wise consumption values, the total fuel consumption over the test cycle run is resulting.

#### Validation

In figure 3.21 the developing of the total fuel consumption [*l*] over time is plotted. Here, the conventional vehicle with the 140 kW SI IC engine in a WLTC is taken as a reference. The continuous line represents the result from Matlab-consumption calculation, whereas the dashed line stands for Dymola-simulation result. As can be seen, the values are matching very well. Nevertheless a little difference can be observed. The result from Matlab calculation is always a little less than Dymola simulation. The accuracy depend on the specific use case and is caused by simplifications made in matlab calculation. In the following the most significant reasons for difference in result are stated:

1. Catalytic heating is not considered.
2. Increased friction during engine heat up is not modeled.
3. Fuel consumption irregularity during an ICE start/stop is not modeled.

### 3 Methodology

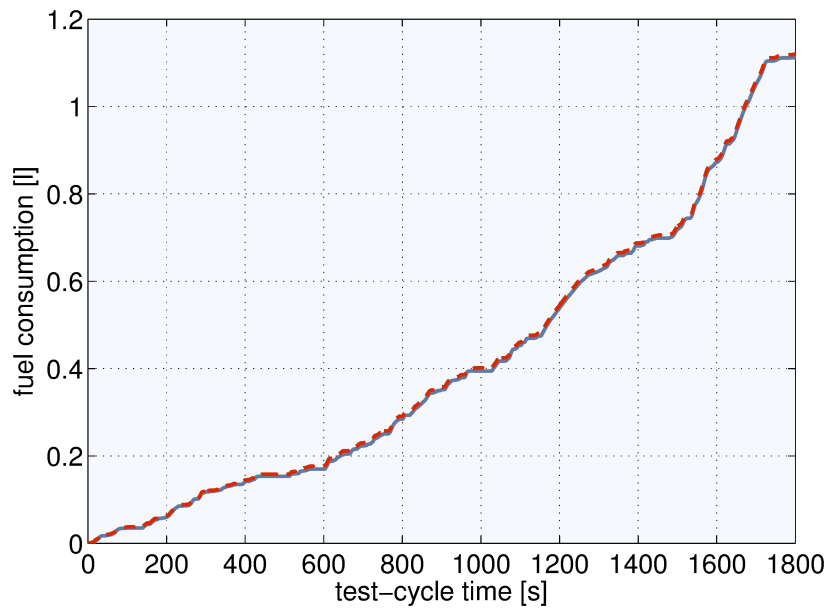


Figure 3.21: Comparison of consumption calculation / Dymola simulation vs. derived Matlab calculation.

Therefore this Matlab-calculation is most accurate when consumption is investigated during stable operation. For the investigated use cases in this work the difference to Dymola simulation varies between 0.5 % and 5 %. However, it needs to be mentioned that the difference between Dymola simulation and the derived Matlab calculation is just relevant for validation purposes. The final results of ICE fuel consumptions are generated by Matlab calculation only. Therefore exactly the same sets of operating points are used to define ICE operation use cases. Comparative investigations based on the same sets of operating points are very accurate.

#### 3.5.2 Reference Simulations as Basis of Valuation

For the analysis of this work clear boundary conditions and use cases need to be specified. By conducting reference simulations, a systematic approach is applied to generate sets of operating points which are building

### 3 Methodology

the basis of valuation.

#### Generating Sets of Operation Points

The simulation signals *effective engine torque* and *engine speed* are the variables which define the specific engine operation (as described in section 3.4.2). Thus, at this point it is crucial to define reference simulations in a way to allow a representative description of ICE engine operation during test run. Hence, the simulation circumstances need to be specified carefully.

First, categories need to be introduced. Figure 3.20 shows some influential factors for the range of operation. In the following an elementary differentiation is stated:

1. Of course, it need to be distinguished between test-runs in different test cycles. For this work the cycles NEDC and WLTC are building the basis of investigation.
2. Since the PHEV operating strategy influences IC engines range of operation, all strategies introduced in section 3.3.3 need to be investigated independently.
3. The power of the compared IC engines has to be of a similar level. Here two power levels are introduced:
  - 100kW IC engine power
  - 140kW IC engine power
4. The full load characteristic needs to be the same or very similar. Otherwise an influence on the selected gears would occur and IC engine's range of operation would be different.
5. Of course SI- and CI IC engines can not be evaluated using the same set of operating points. Therefore the type of IC engine is another category for differentiation.

**Overall Vehicle Specification** To generate the specific ICE operation characteristic a simulation model of conventional vehicle as well as of

### 3 Methodology

PHEV vehicle is used (see section 3.2.1 and refsec:phevvehicle). The three reference IC engines are specified in section 3.2.3.

Each of the two vehicle models are first set-up with the 100kW SI engine, second, with the 140kW SI engine and third, with the 140kW CI engine. Hence, six vehicle configurations are received like shown in table 3.8.

Table 3.8: Motorization of conventional and PHEV vehicle.

	conventional vehicle with	plug-in hybrid vehicle with
Motorization 1	100 kW SI ICE	100 kW SI ICE
Motorization 2	140 kW SI ICE	140 kW SI ICE
Motorization 3	140 kW CI ICE	140 kW CI ICE

**Operation Strategy** For the three PHEV-simulation models, every of the three operating strategies introduced in section 3.3.3 needs to be implemented. Hence, nine PHEV simulation models are resulting.

**Conduction of Reference Simulations** In total 12 vehicle simulation models are defining the reference vehicle specifications. The two test cycles, NEDC and WLTC, are building the use cases. The conventional vehicle models are tested in both cycles. Each operating strategy of PHEV models is just tested in one cycle, since the strategies are bound to a test cycle. After conducting the reference simulations the signals *effective engine torque* and *engine speed* over cycle time can be exported and prepared for further processing.

For useability reasons, the described systematic of calculation has been implemented in a tool, called "Ventus".

#### 3.5.3 Ventus-Tool Environment

Figure 3.22 displays the flow chart of calculation. At the left hand side of the chart the data source is shown. The first data source is the export of

### 3 Methodology

Dymola overall vehicle simulation (upper left corner). The second is the ICE specification introduced by member-files (lower left corner).

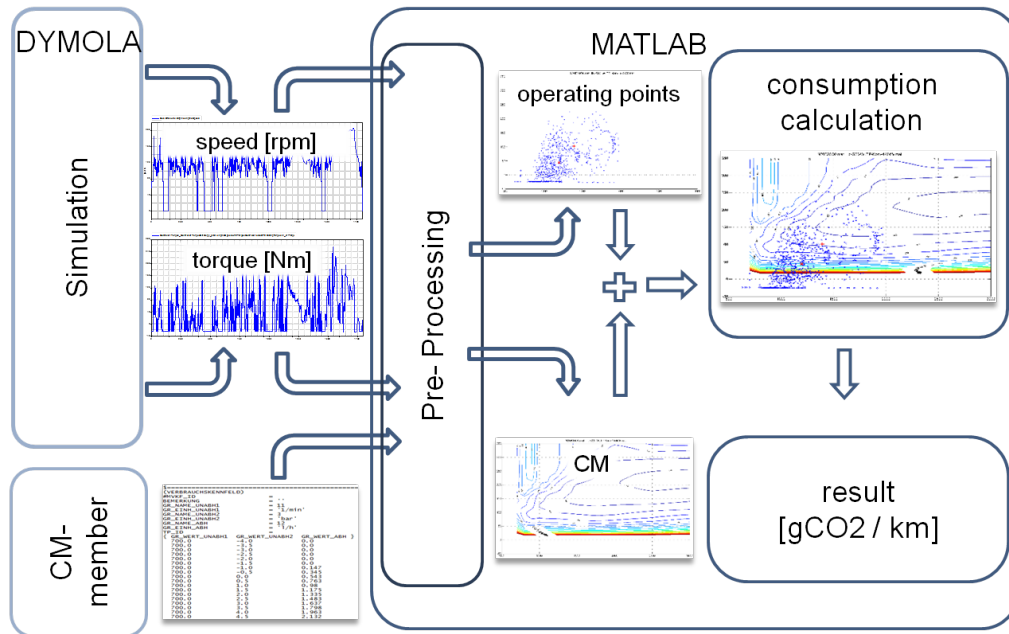


Figure 3.22: Systematic of Matlab consumption calculation.

**Pre-Processor** To generate sets of operating points, the pre-processor reads and converts the signals for *engine speed* and *effective engine torque*. For this task the following steps are conducted:

1. Signals are read in vector form.
2. Units are converted to *rpm* and *Nm*.
3. By the MATLAB command *meshgrid* a two-dimensional data array is created.
4. Axis are defined by engine speed (abscissa) and effective engine torque (ordinate).
5. The operating point of each time-step is integrated in the corresponding array field.
6. The unit of array's values is seconds per field *s*. The sum of all array fields need to be equivalent to the total time of IC engine operation.

### 3 Methodology

The pre-processor for ICE engine consumption maps, reads and transforms data from the ICE member-file. Here the following steps are conducted:

1. Data is read in vector form.
2. By the MATLAB command *meshgrid* a two-dimensional data array is being created.
3. The MATLAB command *griddata* is used to classify all data in this array.
4. Axis are defined by engine speed (abscissa) and effective engine torque (ordinate).
5. Units of the axis are converted to *rpm* and *Nm*.
6. The unit of array's values is *l/h*.

This pre-processing steps are repeated for creation of three libraries: First, the library of sets of operating points. Second, the library of IC engine consumption maps. Third, the library of IC engine  $\Delta$ -consumption maps in percent [%] with respect to the consumption values of a base-consumption map.

**Consumption Calculation** With the data prepared in the pre-processing step and saved in the corresponding library, consumption calculation can be initiated. Therefore the following steps are conducted:

1. An IC engine consumption map which is object of evaluation is selected by the user.
2. A set of operating points is selected with respect to the power class of ICE and the evaluation use case.
3. The data arrays (set of operating points and ICE consumption map) are transformed to the same size. Therefore the MATLAB command *interp2* is applied.
4. Time units of the arrays are transformed into a compatible form.
5. By element wise multiplication of arrays, a data array is received containing field-wise fuel consumption values within the range of operation.
6. By building the sum of all consumption values, the total fuel consumption of the test cycle is resulting.

### 3 Methodology

This systematic can be repeated for another ICE consumption map, keeping the same set of operating points as a basis of valuation. Thus, the consumption values of the two investigated IC engines are measured with exactly the same operation characteristic. The  $\Delta$ -consumption value of these two engines is therefore most accurate.

#### 3.5.4 Features and Benefits

For usability reasons the calculation functions are implemented in a graphical user interface (GUI). All features of Ventus-Tool can be called from one central control panel shown in figure 3.23. As described in the



Figure 3.23: Central control panel of Ventus-Tool.

previous section (3.5.3), vehicle specification as well as the desired use case can be specified by the combination of consumption map and set

### 3 Methodology

of operating points. Therefore the libraries introduced previously, are represented by list-boxes in this central control panel. The upper left list-box displays all consumption maps which are stored in .mat-files in the corresponding library folder. As mentioned these .mat-files can be created by the pre-processor for IC engine consumption maps. The list can be edited freely. The right list-box displays different sets of operating points which are also stored in .mat-file format. The data of these sets are based on the reference Dymola-simulations and computed in the other pre-processing script (also explained in previous section (3.5.3)). The lower left listbox displays the library content of  $\Delta$ -consumption map folder (here empty). In this folder .mat-files are stored, containing  $\Delta$ -consumption maps in percent [%] with respect to a base -consumption map.

#### Consumption Calculation

The user can select a desired combination of consumption- or  $\Delta$ -consumption map on the one hand and a set of operating points on the other hand. By pressing the compute button calculation gets initiated. As a result, a plot with the information stated in the following is received.

- File-name of selected set of operating points and selected ICE consumption map.
- Efficiency map of IC engine.
- Set of operating points.
- The time weighted average (time av) of ICE operation (time av speed and time av torque).
- The consumption weighted average of ICE operation (cons av speed and cons av torque).
- The fuel consumption result of the selected test-run in mass  $CO_2$  per kilometer [ $g_{CO_2}/km$ ].

## 3 Methodology

### Delta Estimations

$\Delta$ -consumption map estimation is a feature for estimating the effect of technological improvements and evaluating their effect. For this function the user can create a  $\Delta$ -consumption map in percent of a base consumption map [%] in excel. Next, Ventus-Tool reads this excel sheet, identifies the table of  $\Delta$ -values as well as the axis. A data array gets created and transformed to the size of a base consumption map. The arrays get matched and a newly generated consumption map is resulting. Figure 3.24 displays the user's interface for  $\Delta$ -estimation. In the upper left listbox a base consumption map can be selected. As already mentioned the input can be defined in the corresponding excel sheet. The pushbutton "renew estimation" triggers the reading process from excel, the array generation and conversion and finally the generation of a new consumption map. In the upper right field the received  $\Delta$ -consumption map from excel is shown. In the lower left field the base consumption map is plotted. In the lower right box the newly generated consumption map is displayed. Whenever the estimation meets user's demand a file-name can be chosen and the new consumption map is saved in the library folder for further investigations.

### Benefits

Next to the original purpose of introducing a calculation method which allow comparative IC engine testing with equal testing conditions, also some other advantages come along. In the following the most important benefits of Ventus-Tool's introduction are stated.

**Equal Testing Conditions and Time Efficiency** Equal testing conditions for comparative ICE testing are achieved by using "frozen" sets of operating points as basis for valuation. Hence, comparative investigations are very accurate.

Furthermore the calculation process is reduced to a minimum. Therefore calculation time is by far shorter than conducting an overall vehicle

### 3 Methodology

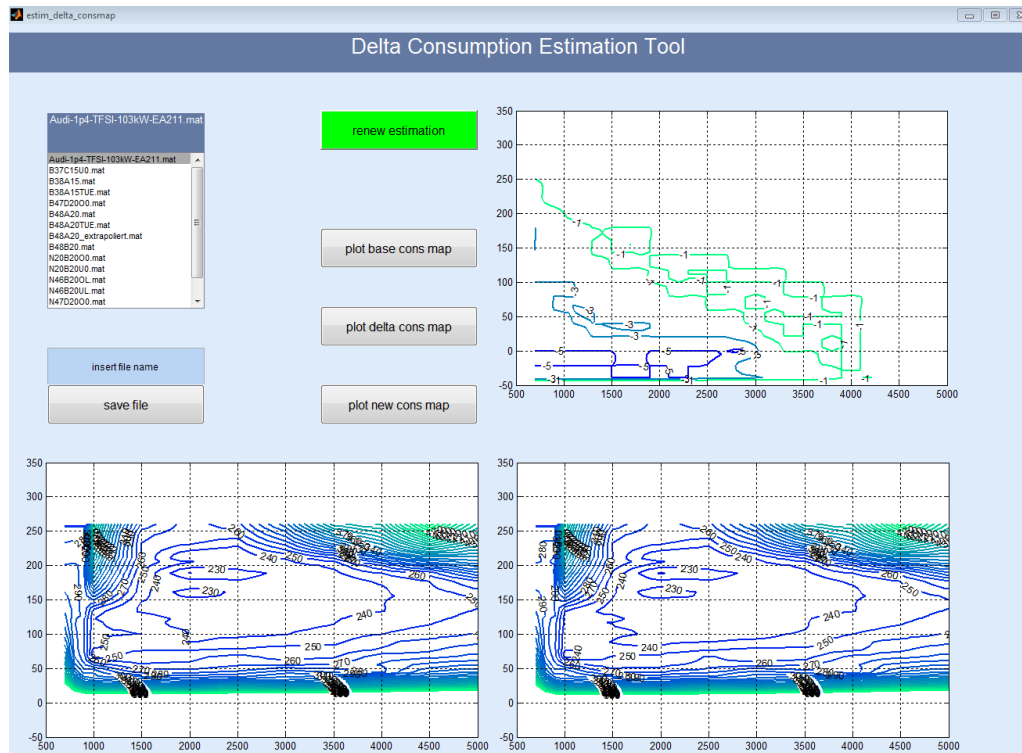


Figure 3.24: Control panel for  $\Delta$ -consumption map estimation.

simulation in Dymola. By using Ventus-Tool environment a variation of similar ICE engines can be conducted in short time.

**PHEV ICE potential potential analysis** The performance of future ICE engine generations are currently investigated very well in conventional vehicles. For PHEV vehicles, these performance predictions are often not existing. Ventus-Tool can be applied to derive future ICE efficiency performance in a PHEV topologies. Since these potentials are usually referred to current IC engines it is easy to conduct a comparative analysis by applying appropriate sets of operating points.

**Estimation of Technological Improvements and Competitors ICE Performance** Presumed that the user has sufficient ICE expertise to do so,

### 3 Methodology

adapptions of base-consumption maps can be conducted easily in an excel spreadsheet. The resulting modified consumption map can be evaluated with little effort by applying sets of operating points for consumption calculation. First, this method can be used to quickly investigate the consequence of consumption map changes due to technological IC engine changes. Second, it enables the possibility to estimate consumption maps of competitors IC engines and to analyze the ICE efficiency potential separately.

## 4 Results

Within this chapter all relevant results of conducted investigations are stated and compared.

Regarding IC engine in PHEV vehicles the following outcomes are stated: First, IC engine operation in PHEV- and conventional drive trains is analyzed with respect to different electric operating strategies and test cycles. Second, the efficiency performance of different IC engine generations is compared within the drive trains of the two vehicle concepts in different test cycles.

Regarding gearbox analysis in PHEV vehicles the following is discussed: First, the potential of efficiency improvements for the PHEV vehicle and respectively, the conventional vehicle is discussed. Second, the effect of a decrease of gear number and changed gear-stepping is investigated for the two vehicle concepts.

### 4.1 IC Engine in Parallel Hybrid Vehicles

#### 4.1.1 Analysis of Operating Pattern

In this section some elementary values which define IC engine's operation during a test-cycle-run are stated. The selected values are:

- Distribution of ICE's operating range described by plotted operating points.
- Duration of IC engine operation while test-cycle-run.
- Number of engine starts during test-run.

## 4 Results

- Time-weighted average of engine speed and effective engine torque (time-weighted av torque/speed).
- Consumption-weighted average of engine speed and effective engine torque (cons-weighted av torque/speed).

In the following ICE operation with different PHEV electric operating strategies (introduced in section 3.3.3) are compared cycle-wise. As a reference also ICE operation in the conventional vehicle is stated. Of course the different engine power levels (introduced in section 3.2.3) cause differing ICE operating patterns. During investigation, it has been observed that the distribution of operating points of the different motorizations is developing in a similar way with a change of use case. Therefore, just the operating patterns resulting of the 140 kW SI motorization are highlighted. The following the characteristic values of ICE engine operation in the different use cases are stated. These values are derived from Dymola-simulation results of the vehicles models as specified in section 3.2.

### Operating Pattern in NEDC

**Conventional Vehicle** The range of operation of the 140 kW SI IC engine in the conventional vehicle in NEDC is displayed in figure 3.13. In table 4.1 selected characters are listed, which describe the specific operation behavior.

Table 4.1: IC engines range of operation / conventional vehicles in NEDC.

		100 kW SI	140 kW SI	140 kW CI
Duration of operation	[s]	946	943	927
Number of ICE starts		12	12	13
Time-weighted av speed	[rpm]	1095	1072	1181
Time-weighted av torque	[Nm]	33,5	32,7	32,9
Cons-weighted av speed	[rpm]	1281	1238	1354
Cons-weighted av torque	[Nm]	74,3	76,8	74,1

## 4 Results

**PHEV eOS 1** The range of operation of the 140 kW SI IC engine in the PHEV vehicle with eOS 1 in NEDC is displayed in figure 3.15. In table 4.2 selected characters are listed, which describe the specific operation behavior. Here, the following assumptions can be made:

- The duration of PHEV's ICE operation is just about 40 % of the duration in conventional vehicle. Since this is defined by the operating strategy there is no significant difference between IC engines.
- The increase of engine torque's time-weighted average is more than 130 % for the two SI motorizations and about 210 % for the CI IC engine.
- The increase of engine speed's time-weighted average is about 45 % for the two SI motorizations and 25 % for the CI IC engine.

Table 4.2: IC engines range of operation / PHEV with eOS 1 in NEDC.

		100 kW SI	140 kW SI	140 kW CI
Duration of operation	[s]	397	397	344
Number of ICE starts		10	10	10
Time-weighted av speed	[rpm]	1571	1572	1486
Time-weighted av torque	[Nm]	77,3	80,2	103,2
Cons-weighted av speed	[rpm]	1677	1680	1511
Cons-weighted av torque	[Nm]	113,1	119,7	129,8

**PHEV eOS 2** The range of operation of the 140 kW SI IC engine in the PHEV vehicle with eOS 2 in NEDC is displayed in figure 3.16. In table 4.3 selected characters are listed, which describe the specific operation behavior. Since this electric operating strategy is just evaluated as a reference, only the operation of 140 kW SI engine has been modeled in Dymola-simulation. Here, the following assumptions can be made:

- The duration of PHEV's ICE operation is just about 26 % of the duration in conventional vehicle.
- The increase of engine torque's time-weighted average is about 320 %.
- The increase of engine speed's time-weighted average is about 60 %.

## 4 Results

Table 4.3: IC engines range of operation / PHEV with eOS 2 in NEDC.

		140 kW SI
Duration of operation	[s]	245
Number of ICE starts		2
Time-weighted av speed	[rpm]	1685
Time-weighted av torque	[Nm]	137,1
Cons-weighted av speed	[rpm]	1696
Cons-weighted av torque	[Nm]	155,2

### Operating Pattern in WLTC

**Conventional Vehicle** The range of operation of the 140 kW SI IC engine in the conventional vehicle in WLTC is displayed in figure 3.14. In table 4.4 selected characters are listed, which describe the specific operation behavior.

Table 4.4: IC engines range of operation / conventional vehicles in WLTC.

		100 kW SI	140 kW SI	140 kW CI
Duration of operation	[s]	1594	1592	1593
Number of ICE starts		7	7	8
Time-weighted av speed	[rpm]	1225	1195	1267
Time-weighted av torque	[Nm]	42,8	44,0	42,5
Cons-weighted av speed	[rpm]	1494	1396	1461
Cons-weighted av torque	[Nm]	95,7	102,6	100,9

**PHEV eOS 3** The range of operation of the 140 kW SI IC engine in the PHEV vehicle with eOS 3 in WLTC is displayed in figure 3.17. In table 4.5 selected characters are listed, which describe the specific operation behavior. Here, the following assumptions can be made:

- The duration of PHEV's ICE operation is about 45 % of the duration in conventional vehicle. Since this is defined by the operating strategy there is no significant difference between IC engines.

## 4 Results

- The increase of engine torque's time-weighted average is about 90 % for the two SI motorizations and about 130 % for the CI IC engine.
- The increase of engine speed's time-weighted average is about 40 % for the two SI motorizations and 20 % for the CI IC engine.

Table 4.5: IC engines range of operation / PHEV with eOS 3 in WLTC.

		100 kW SI	140 kW SI	140 kW CI
Duration of operation	[s]	770	769	726
Number of ICE starts		33	33	34
Time-weighted av speed	[rpm]	1686	1665	1542
Time-weighted av torque	[Nm]	83,2	85,0	99,6
Cons-weighted av speed	[rpm]	1816	1752	1622
Cons-weighted av torque	[Nm]	119,2	122,4	134,9

### 4.1.2 Evaluation of IC Engine Generations

In this section IC engine's efficiency performance over different engine generations is stated. As mentioned in the beginning, these ICE generations were originally developed for conventional application. Evaluation is conducted in the PHEV vehicle (specified in section 3.2.2) and, in order to provide a reference, in the conventional vehicle (characterized in section 3.2.1). For ICE's efficiency performance the value of guidance is IC engines carbon dioxide emission per kilometer [ $gCO_2/km$ ]. This value is evaluated over one test-run in a cycle of NEDC or WLTC. Detailed conditions for evaluation are stated in section 3.3. For this investigation specific IC engines are selected to represent the characteristic of each generation. In the following these generation representing ICEs are introduced.

#### 100 kW SI IC Engine Generations

For the 100 kW SI ICE category the following engines have been selected:

## 4 Results

**Previous generation** Here the previous generation is represented by naturally aspirated 4 cylinder engine. Data concerning this engine is listed in table 4.6.

Table 4.6: IC engine specification of 100 kW SI engine class / previous generation.

Production time	2004 – 2007
Layout	4 cylinders, in-line
Charging	naturally aspirated
Displacement	1995 $cm^3$
Power	95 kW at 5750 rpm
Torque	180 Nm at 3250 rpm
Compression	10,5 : 1
Bore diameter / stroke	84 mm x 90 mm

**Current generation** The current generation of this category is represented by a 1,5 liter 3 cylinder turbo- and a 1,4 liter 4 cylinder turbo engine. Specific data is listed in table 4.7 for the 1,5 liter 3 cylinder engine and in table 4.8 for the 1,4 liter 4 cylinder engine.

Table 4.7: IC engine specification of 100 kW SI IC engine class / current generation (3-cylinder).

Production time	since 2014
Layout	3 cylinders, in-line
Charging	turbo charged
Displacement	1499 $cm^3$
Power	100 kW at 4400 rpm
Torque	220 Nm at 1250 rpm
Compression	11,0 : 1
Bore diameter / stroke	82 mm x 94,6 mm

**Next generation** Next generation is represented by a revised edition of the 3 cylinder turbo engine of current generation. The following data is

## 4 Results

Table 4.8: IC engine specification of 100 kW SI IC engine class / current generation (4-cylinder).

Production time	since 2014
Layout	4 cylinders, in-line
Charging	turbo charged
Displacement	1395 $cm^3$
Power	103 kW at 4500 rpm
Torque	250 Nm at 1500 rpm
Compression	10,0 : 1
Bore diameter / stroke	74,5 mm x 80,0 mm

based on the assumption that the basic configuration does not change. Data concerning this engine is listed in table 4.9.

Table 4.9: IC engine specification of 100 kW SI IC engine class / next generation.

Production time	from 2016
Layout	3 cylinders, in-line
Charging	turbo charged
Displacement	1499 $cm^3$
Power	100kW at 4400rpm
Torque	220Nm at 1250rpm
Compression	11,0 : 1
Bore diameter / stroke	82mm x 94,6mm

### Evaluation of 100 kW SI IC Engines

Analysis of this section has been conducted respectively to the PHEV and conventional vehicle, specified in section 3.2 in NEDC. Before stating results, the charts, shown in figure 4.1, 4.2 and 4.3, is explained within the subsequent paragraph.

**Chart explanation** The chart shows differences of carbon dioxide emissions of three IC engine generations. Each generation is placed in one

## 4 Results

column.  $\Delta$ -values of the previous and the next generation are given with respect to  $CO_2$ -emission of the current generation's IC engines. The horizontal displacement within the marked columns arose out of visual clearness-reasons and is not indicating any information concerning investigated IC engines. The two horizontally displaced  $\Delta$ -consumption values in each column, are representing ICE's operation in conventional vehicle and in PHEV vehicle. As indicated in chart's legend,

- the dashed line connects all  $\Delta$ - values of conventional operation,
- the chain-dotted line connects all  $\Delta$ - values of PHEV operation with eOS 1 for NEDC and eOS 3 for WLTC,
- the dotted line in some NEDC charts connects all  $\Delta$ - values of PHEV operation with eOS 2.

**In NEDC** The chart in top of figure 4.1 shows carbon dioxide emissions of different IC engine generations of the 100 kW SI IC engine class in NEDC. Here, the current generation is represented by two IC engines with a consumption difference of approximately  $2 \text{ gCO}_2/\text{km}$ , summed up in vertical ellipses. Since emission differences are illustrated relatively to the current IC engine generation the center-points of ellipses are placed at the zero-line.

It can be seen that the previous generation IC engine performs far better in PHEV drive train than in the conventional one. Furthermore it can be read that next generations efficiency measures cause significantly greater improvements within the conventional drive train operation than in PHEV operation.

**In WLTC** The chart in bottom of figure 4.1 shows carbon dioxide emissions of different IC engine generations of the 100 kW SI IC engine class in WLTC.

In general in the WLTC use case the same tendencies as in NEDC can be observed. However, the difference of efficiency performance of previous generation IC engine is here even greater.

## 4 Results

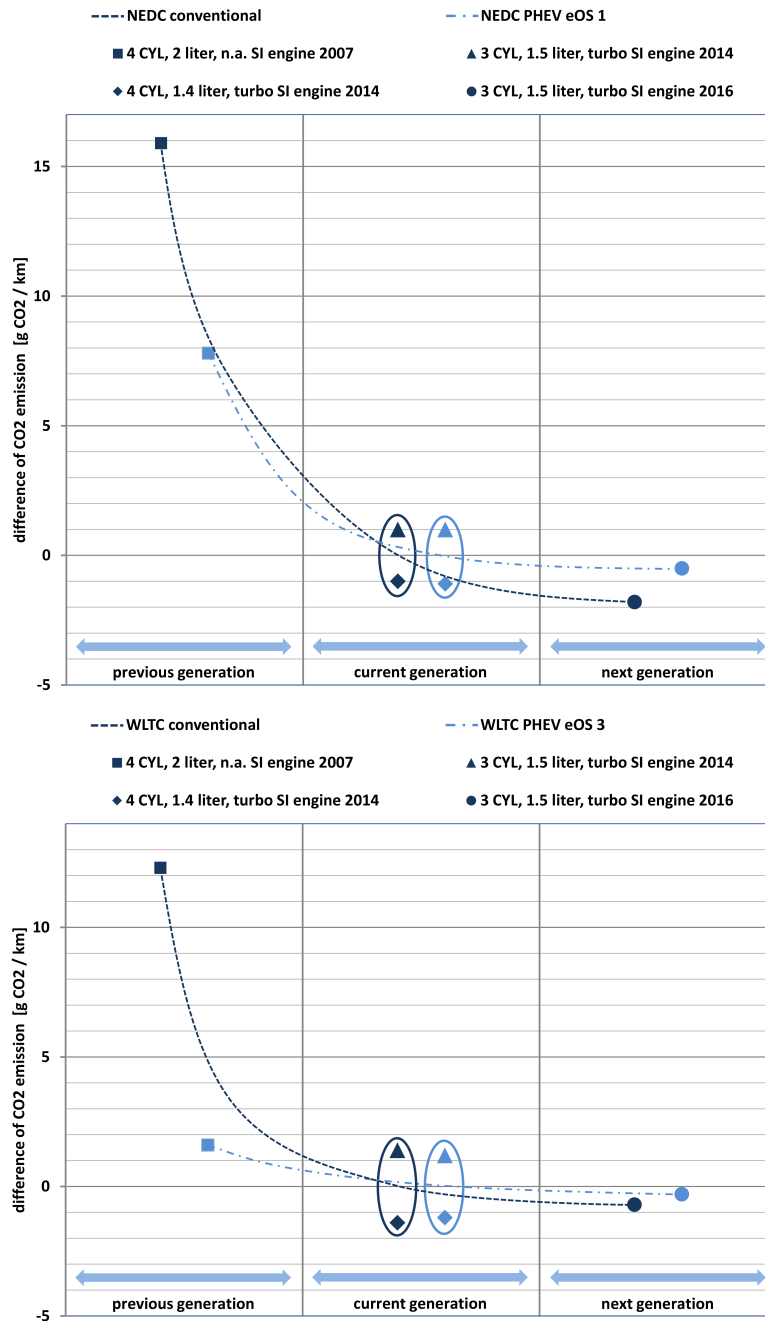


Figure 4.1: Top: CO<sub>2</sub> reduction over IC engine generations / 100kW SI IC engines in NEDC.  
Bottom: CO<sub>2</sub> reduction over IC engine generations / 100kW SI IC engines in WLTC.

## 4 Results

### Introduction of 140 kW SI IC Engine Generations

For the 140kW SI category the following engines have been selected:

**Previous generation** Here the previous generation is represented by a 2 liter, 4 cylinder turbo engine from 2011. Data concerning this engine is listed in table 4.10.

Table 4.10: IC engine specification of 140 kW SI IC engine class / previous generation.

Production time	since 2011
Layout	4 cylinders, in-line
Charging	turbo charged
Displacement	1997 $cm^3$
Power	135 kW at 5000 rpm
Torque	270 Nm at 1250 rpm
Compression	11,0 : 1
Bore diameter / stroke	84 mm x 90,1 mm

**Current generation** The current generation of this category is represented by a 2 liter, 4 cylinder turbo engine from 2011. Data concerning this engine is listed in table 4.11.

Table 4.11: IC engine specification of 140 kW SI IC engine class / current generation.

Production time	since 2014
Layout	4 cylinders, in-line
Charging	turbo charged
Displacement	1998 $cm^3$
Power	141 kW at 4700 rpm
Torque	280 Nm at 1250 rpm
Compression	11,0 : 1
Bore diameter / stroke	82 mm x 94,6 mm

## 4 Results

**Next generation** Next generation is represented by a new edition of the previous 4 cylinder turbo engine. The following data is based on the assumption that the basic configuration does not change. Data concerning this engine is listed in table 4.12.

Table 4.12: IC engine specification of 140 kW SI IC engine class / next generation.

Production time	from 2016
Layout	4 cylinders, in-line
Charging	turbo charged
Displacement	1998 $cm^3$
Power	141 kW at 4700 rpm
Torque	280 Nm at 1250 rpm
Compression	11,0 : 1
Bore diameter / stroke	82 mm x 94,6 mm

### Evaluation of 140 kW SI IC Engines

**In NEDC** The chart in top of figure 4.2 shows carbon dioxide emissions of different IC engine generations of the 140 kW SI IC engine class in NEDC.

Here, it can be observed that emission difference over generations behaves in a rather similar way. Just next generation's IC engine is showing little difference. The more load-points are shifting towards higher load areas, the less of CO<sub>2</sub> difference can be realized.

**In WLTC** The chart in the bottom of figure 4.2 shows carbon dioxide emissions of different IC engine generations of the 140 kW SI IC engine class in WLTC.

Here, IC engines efficiency performance in the PHEV- and the conventional drive train behaves rather similar.

## 4 Results

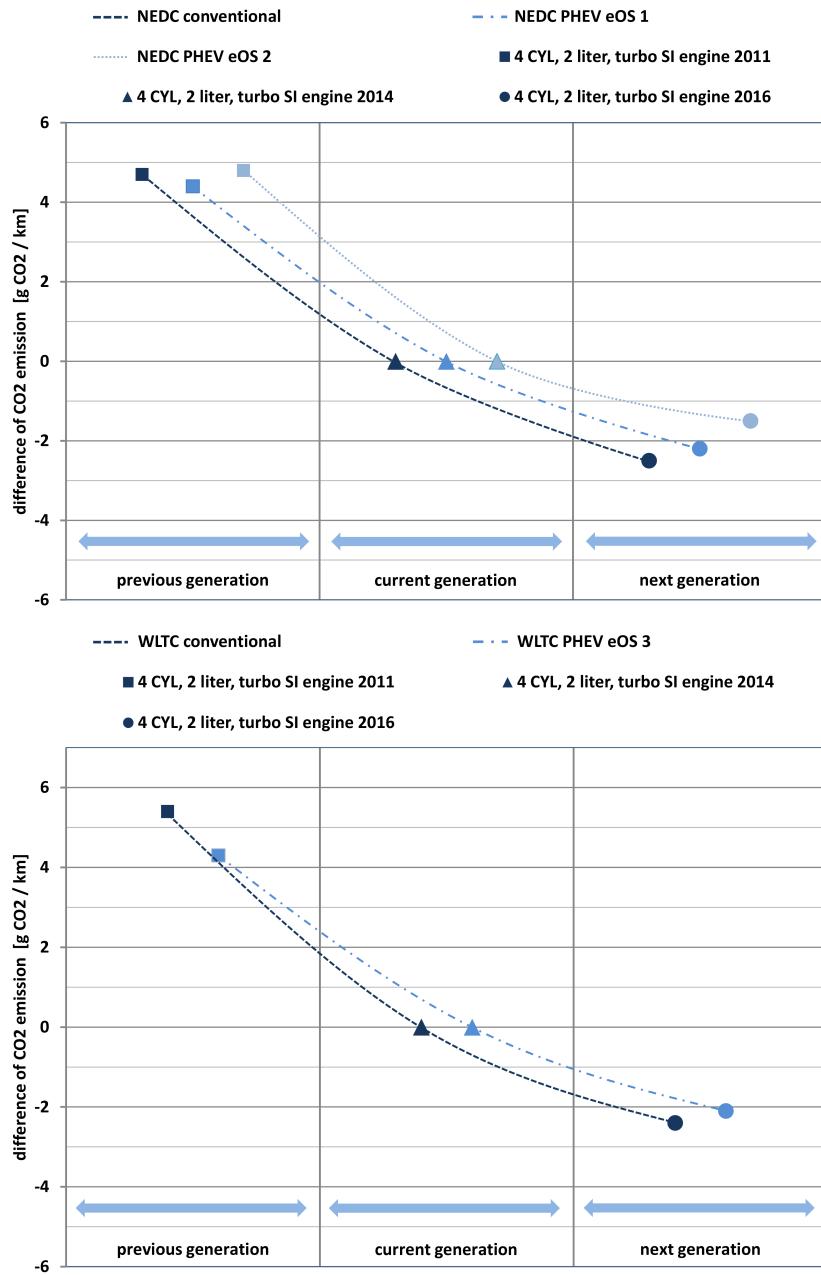


Figure 4.2: Top: CO<sub>2</sub> reduction over IC engine generations / 140kW SI IC engines in NEDC.  
 Bottom: CO<sub>2</sub> reduction over IC engine generations / 140kW SI IC engines in WLTC.

## 4 Results

### Introduction of 140 kW Diesel IC Engine Generations

For the 140kW CI<sup>1</sup> category just two engine generations were investigated:

**Previous generation** Here the previous generation is represented by a 2 liter, 4 cylinder turbo Diesel engine from 2010. Data concerning this engine is listed in table 4.13.

Table 4.13: IC engine specification of 140 kW CI IC engine class / previous generation.

Production time	since 2010
Layout	4 cylinders, in-line
Charging	turbo charged
Displacement	1995 $cm^3$
Power	135 kW at 4000 rpm
Torque	380 Nm at 1750 rpm
Compression	16,5 : 1
Bore diameter / stroke	84 mm x 90 mm

**Current generation** The current generation of this category is represented by a 2 liter, 4 cylinder turbo Diesel engine from 2014. Data concerning this engine is listed in table 4.14.

### Evaluation of 140 kW CI IC Engines

**In NEDC** The chart in top of figure 4.3 shows carbon dioxide emissions of different IC engine generations of the 140 kW CI IC engine class in NEDC.

Here, a significant difference of efficiency performance can be observed. The following conclusion can be derived. The more IC engine is operated

---

<sup>1</sup>Compression Ignited

## 4 Results

Table 4.14: IC engine specification of 140 kW CI IC engine class / current generation.

Production time	since 2014
Layout	4 cylinders, in-line
Charging	turbo charged
Displacement	1998 $cm^3$
Power	140 kW at 4000 rpm
Torque	400 Nm at 1750 rpm
Compression	16,5 : 1
Bore diameter / stroke	84 mm x 90 mm

in areas of greater load, the less efficiency gain can be realized by this generation change.

**In WLTC** The chart in the bottom of figure 4.3 shows carbon dioxide emissions of different IC engine generations of the 140 kW CI IC engine class in WLTC.

## 4.2 Gearbox in Parallel Hybrid Vehicles

In this section the following steps are conducted: First, PHEV specific gearbox use of the configuration, introduced in section 3.2.2, is investigated. Second, the potential of recuperative power flow passing through transmission during a NEDC and WLTC test-run is analyzed. Finally, a sensitivity analysis regarding reduction of friction in transmission is made.

### 4.2.1 Gearbox Operation

Since the recuperative energy needs to pass transmission from vehicle to electric machine (described in section 3.1.2), the gearbox is transmitting greater power flows, relevant for overall efficiency of vehicle operation.

## 4 Results

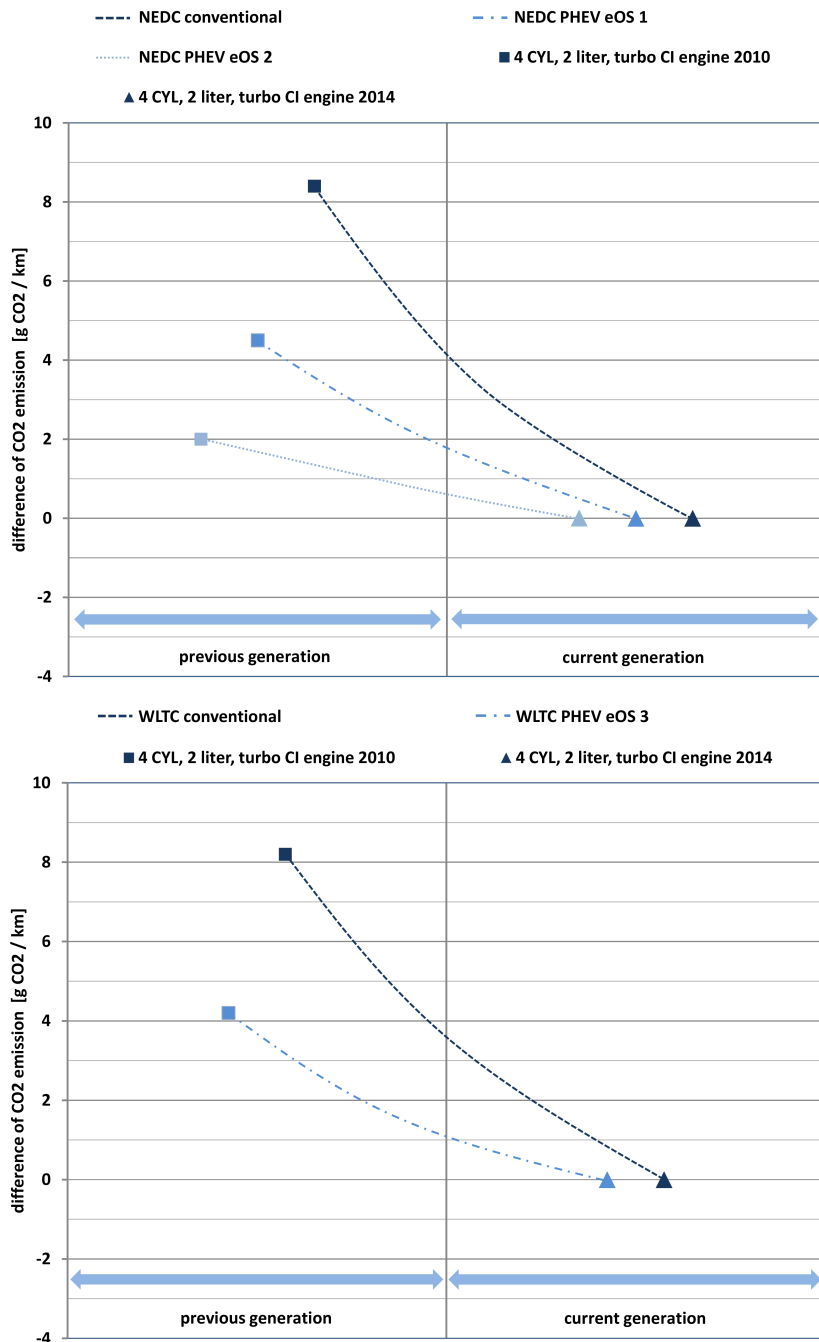


Figure 4.3: Top: CO<sub>2</sub> reduction over IC engine generations / 140kW CI IC engines in NEDC.  
 Bottom: CO<sub>2</sub> reduction over IC engine generations / 140kW CI IC engines in WLTC.

## 4 Results

### Propulsion Power and Energy

In order to drive a vehicle through test cycle's velocity profile, the necessary propulsion power needs to be transmitted by the drive train. The two charts in figure 4.4 display the developing of propulsion power, traction- and breaking energy. These measures are derived from vehicle simulation in NEDC and WLTC of the PHEV vehicle. The mathematical description can be found in section 3.1.

1. Propulsion power  $P_{prop}(t)$  over time is indicated by the continuous line on the left scale.
2. Positive traction energy  $E_{trac}(t)$  over time is represented by the dashed line on the upper right scale.
3. Negative breaking energy  $E_{break}(t)$  is shown by the dotted line on the lower right scale. In the periods of breaking recuperation can be conducted. Hence, the value of total breaking energy can be seen as the theoretical potential for recuperation.

**Propulsion Power and Energy in NEDC** The top of figure 4.4 shows the developing of values described above, while running through a NEDC profile. It can be seen that the drive train is transmitting 1,2 kWh for traction and -0,5 kWh for breaking.

**Propulsion Power and Energy in WLTC** The bottom of figure 4.4 shows the developing of the introduced values, while running through a WLTC profile. Here, it can be read that the drive train is transmitting 3,2 kWh for traction and -1,2 kWh for breaking.

### 4.2.2 Potential of Friction Reducing Measures

As already mentioned vehicle's movement through a test-cycle causes a significant amount of breaking energy. A part of this energy can be used for recuperation and is therefore increasing overall vehicle's efficiency during a test-run.

## 4 Results

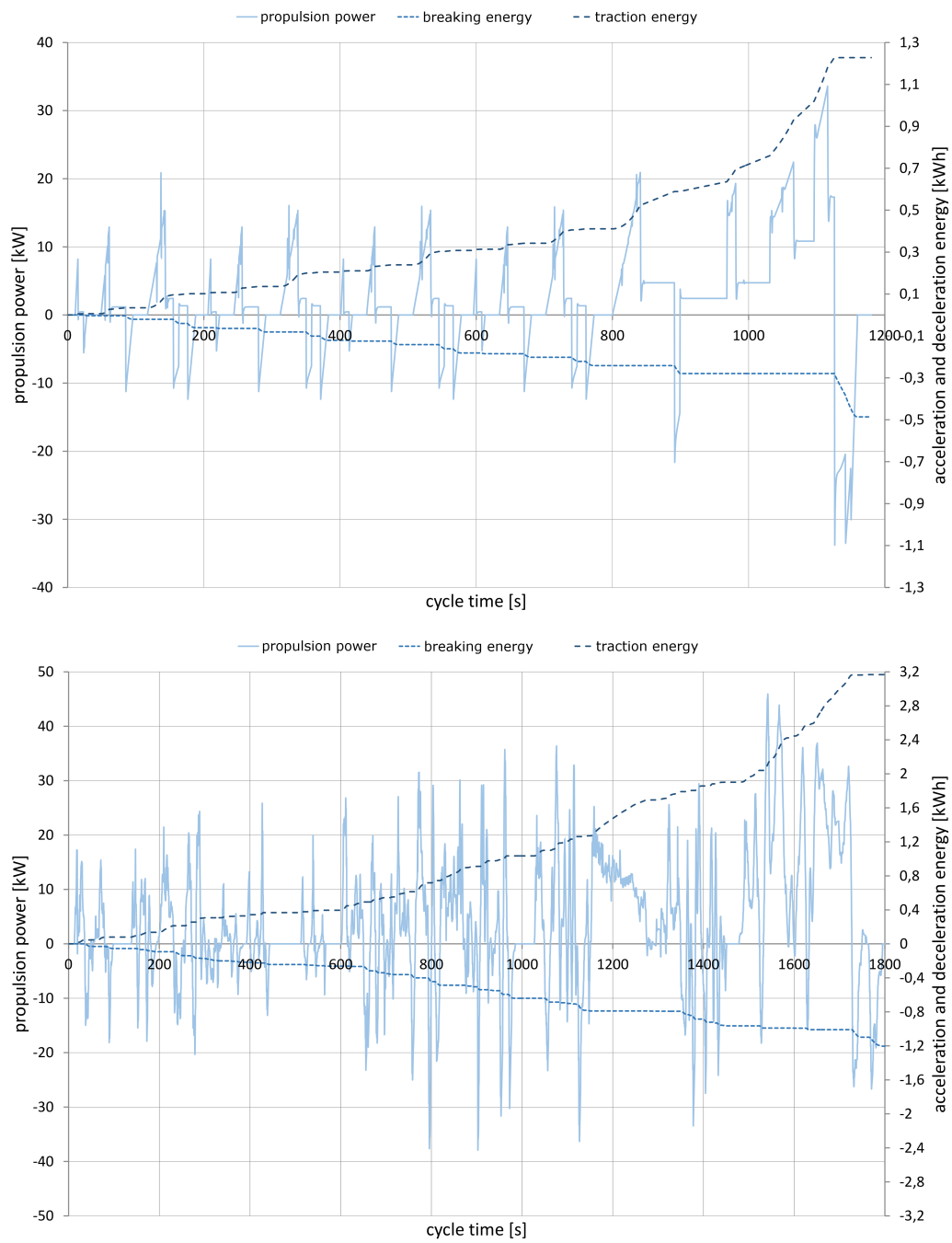


Figure 4.4: Propulsion power and energy of PHEV vehicle in NEDC & WLTC.

## 4 Results

In section 3.4.3, the dependency of gearbox friction torque on speed, input torque, the selected gear and gearbox temperature is described. For this analysis a constant value of transmission efficiency is assumed, regardless of the current speed, the selected gear and gearbox temperature. Hence, friction torque is modeled with a linear dependency on input torque. The friction of idling is considered by the integration of driving resistance values in the longitudinal vehicle model. [23]

Here, the three chosen values for constant efficiency are: 94 %, 96 %, 98 %.

The chart in the top of figure 4.5 shows the reducing effect on carbon dioxide emissions due to an increase of transmission efficiency in NEDC. The trend of this chart shows that friction torque reduction leads to a greater effect in the PHEV vehicle rather than in the conventional one. The difference is about 20 %.

The chart in the bottom of figure 4.5 shows the reducing effect on carbon dioxide emissions due to an increase of transmission efficiency in WLTC. The trend of this chart shows that friction torque reduction leads to a greater effect in the PHEV vehicle rather than in the conventional one. Here, the difference is about 25 %. The extra difference compared to NEDC test-run can be explained by the characteristic of WLTC. This test-cycle is providing more potential for recuperation than NEDC.

## 4 Results

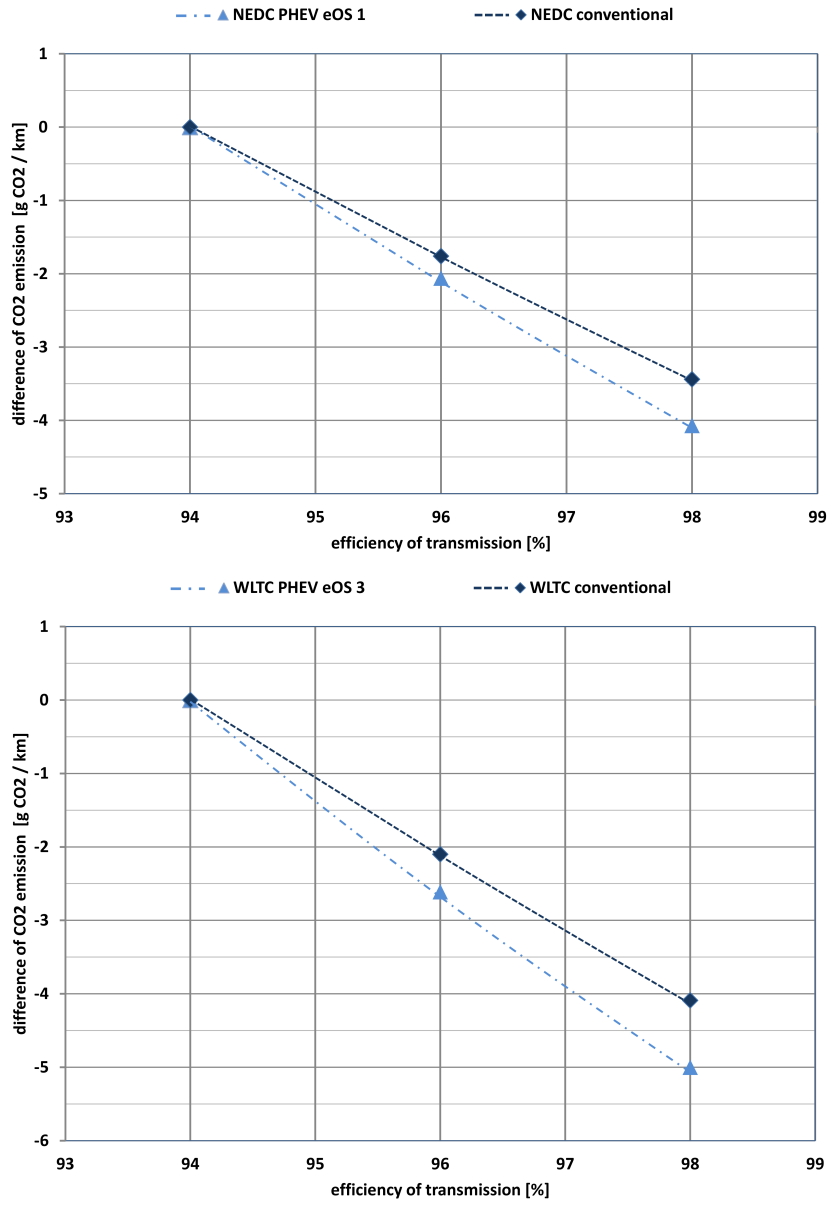


Figure 4.5: Top: CO<sub>2</sub> reduction over gearbox efficiency increase in NEDC.  
Bottom: CO<sub>2</sub> reduction resulting of gearbox efficiency increase in WLTC.

## 5 Conclusions

At the outset of this work was the central question: *"To what extent plug-in hybrid vehicles can benefit from components, originally developed for conventional applications?"* It was objective to contributing in building a solid basis for car manufacturers product decision making process regarding the subsystems *internal combustion engine* and *gearbox*.

**Subsystem IC Engine** First, an analysis of PHEV specific IC engine operation was conducted. Therefore a parallel plug-in hybrid D-segment vehicle was selected as a concept platform. Tests were conducted in state-of-charge minimum mode, applying 3 different electric operating strategies. As use cases the driving cycles NEDC and WLTC were chosen.

It was demonstrated that IC engine operation in PHEV vehicles has a strong dependency on the electric operating strategy and the driving cycle. By applying different strategies ICE operation time was reduced by 55 % to 75 % compared to conventional vehicle. IC engine's average speed increased by 20 % to 60 % and effective engine torque increased by 90 % to 320 %.

The gain of efficiency performance of different IC engine generations in PHEV vehicle was analyzed by applying a specifically developed calculation method. This Matlab based algorithm is using signals for *engine speed* and *engine torque* from a reference simulation. With these input characters a sets of operating points is created as a specification of operation for comparative investigations. Here a quick and very accurate investigation method for testing of similar IC engines was found.

## 5 Conclusions

For the ICE categories 100 kW spark ignited, 140 kW spark ignited and 140 kW compression ignited an analysis of different generations was conducted. Whereas investigated IC engines were originally developed for conventional application. Here, the tendency was observed that the reduction of carbon dioxide emissions due to a new engine generation is more distinctive in conventional drive trains rather than in PHEV drive trains. It was observed that PHEV efficiency benefits significantly less from the step - naturally aspirated spark ignition engine to state of the art turbo engine - than conventional vehicle. 55 % of of conventional vehicle's total CO<sub>2</sub> reduction can be realized in PHEV in NEDC and only 13 % of it can be realized in WLTC.

**Subsystem Gearbox** The selected PHEV drive train causes that all recuperative energy flow from vehicle towards the electric machine passes through transmission. Hence, also during vehicle's breaking phases, the gearbox conveys energy, relevant for overall vehicle efficiency. By applying vehicle simulation the PHEV specific use of drive train was analyzed. In NEDC and WLTC the potential for recuperation is about 40 % of total propulsion power.

A sensitivity analysis regarding reduction of friction losses in transmission was conducted. It was observed that the effect of reduction of friction losses in transmission is more distinctive for PHEV drive trains rather than conventional drive trains. In NEDC an increase of transmission efficiency causes 20 % more CO<sub>2</sub> reduction in PHEV compared to conventional vehicle. In WLTC the difference is 25 %.

# Bibliography

- [1] European Environment Agency. *Average emissions for new cars (gCO<sub>2</sub>/km)*. 2005. URL: <http://www.eea.europa.eu/data-and-maps/figures/average-emissions-for-new-cars/average-emissions-for-new-cars> (visited on 09/12/2015) (cit. on p. 1).
- [2] Christoph Clauss et al. *Mixed-Domain Modeling in Modelica*. first. Springer US, 2004. ISBN: 0-306-48734-9 (cit. on p. 38).
- [3] Dieter Schramm et al. *Vehicle Dynamics- Modeling and Simulation*. second. Springer, 2014. ISBN: 978-3-540-36044-5 (cit. on p. 38).
- [4] Franz Mayinger et al. *Mobility and Traffic in the 21st Century*. first. Springer, 2001. ISBN: 978-3-662-04392-9 (cit. on p. 1).
- [5] Heinz Schäfer et al. *Trends in der elektrischen Antriebstechnologie für Hybrid- und Elektrofahrzeuge*. Expert, 2012. ISBN: 978-3-8169-3100-3 (cit. on p. 6).
- [6] Reiner Korthauer et al. *Handbuch Elektromobilität*. First Edition. 2010 (cit. on p. 24).
- [7] Susan Solomon et al. "Irreversible climate change due to carbon dioxide emissions." In: *Proceedings of the National Academy of Sciences* (Feb. 2009), pp. 1704–1709 (cit. on p. 1).
- [8] Richard Backhaus. "Trends in der Antriebstechnik." In: *Motortechnische Zeitschrift* (Sept. 2009), pp. 618–625 (cit. on p. 2).
- [9] Beuth. *DIN 70020-3*. 2008. URL: <http://www.beuth.de/de/norm/din-70020-3/92396851> (visited on 08/20/2015) (cit. on p. 7).
- [10] BMW. *BMW i3*. 2015. URL: <http://www.bmw.at/de/neufahrzeuge/bmw-i/i3/2013/start.html> (visited on 09/11/2015) (cit. on pp. 7, 8).

## Bibliography

- [11] BMW. *Corporate News*. 2015. URL: [http://www.bmwgroup.com/d/0\\_0\\_www\\_bmwgroup\\_com/investor\\_relations/corporate\\_news/news/2015/vertriebsmeldung\\_januar2015.html](http://www.bmwgroup.com/d/0_0_www_bmwgroup_com/investor_relations/corporate_news/news/2015/vertriebsmeldung_januar2015.html) (visited on 09/12/2015) (cit. on p. 22).
- [12] BMW. *ZUKUNFTSWEISENDE MOBILITÄT DANK BMW eDRIVE*. 2015. URL: <http://www.bmw.at/de/topics/faszination-bmw/efficientdynamics/edrive.html> (visited on 09/12/2015) (cit. on pp. 6, 7).
- [13] BMW-Group. *B38A15Mo*. 2015. URL: <http://www.bmwarchiv.de/m-code/b38a15m0.html> (visited on 05/09/2015) (cit. on p. 25).
- [14] BMW-Group. *B47D20Oo*. 2015. URL: <http://www.bmwarchiv.de/m-code/b47d20o0-140.html> (visited on 10/09/2015) (cit. on p. 25).
- [15] BMW-Group. *B48A20Mo*. 2015. URL: <http://www.bmwarchiv.de/m-code/b48a20m0.html> (visited on 05/09/2015) (cit. on p. 25).
- [16] Chevrolet. *Volt*. 2015. URL: <http://www.chevrolet.com/volt-electric-car.html> (visited on 08/09/2015) (cit. on p. 9).
- [17] VIII Biennial Asilomar Conference. *Transportation, Energy, and Environmental Policy*. 2001 (cit. on p. 22).
- [18] Markus Duesmann. "Warum sich e-Antriebe durchsetzen." In: *Motortechnische Zeitschrift* (June 2014), pp. 54–59 (cit. on pp. 2, 3).
- [19] EEA. *Monitoring CO<sub>2</sub> emissions from passenger cars and vans in 2013*. European Environment Agency, 2014 (cit. on p. 1).
- [20] Fisker. *Fisker Karma*. 2015. URL: <http://www.fisker-automobile.com/?id=126> (visited on 09/11/2015) (cit. on p. 7).
- [21] Ford. *C-MAX Energi*. 2015. URL: <http://www.ford.com/cars/cmax/trim/energi/> (visited on 08/09/2015) (cit. on p. 9).
- [22] Lino Guzzela and Antonio Sciarretta. *Vehicle Propulsion Systems-Introduction to Modeling and Optimization*. second. Springer, 2013. ISBN: 978-3-642-35913-2 (cit. on pp. 6, 12–14, 16–20, 40).
- [23] Peter Hofmann. *Hybridfahrzeuge Ein alternatives Antriebssystem für die Zukunft*. second. Springer, 2014. ISBN: 978-3-7091-1780-4 (cit. on pp. 2, 6, 24, 73).

## Bibliography

- [24] Mercedes-Benz. *Konfigurator*. 2015. URL: [http://www.mercedes-benz.at/content/austria/mpc/mpc\\_austria\\_website/de/home\\_mpc/passengercars/home/new\\_cars/models/s-class/w222.flash.html](http://www.mercedes-benz.at/content/austria/mpc/mpc_austria_website/de/home_mpc/passengercars/home/new_cars/models/s-class/w222.flash.html) (visited on 08/19/2015) (cit. on pp. 6, 7).
- [25] Mitsubishi. *Outlander PHEV*. 2015. URL: <http://www.mitsubishi-motors.at/outlander-phev/> (visited on 08/20/2015) (cit. on p. 9).
- [26] Audi Österreich. *Audi A3 Sportback e-tron*. 2015. URL: [https://www.audi.at/modelle/audi\\_tron/a3\\_sportback\\_e\\_tron/technische\\_daten/](https://www.audi.at/modelle/audi_tron/a3_sportback_e_tron/technische_daten/) (visited on 08/09/2015) (cit. on pp. 6, 7).
- [27] Stefan Pischinger. "Optimierte Auslegung von Ottomotoren in Hybrid-Antriebssträngen." In: *Motortechnische Zeitschrift* (July 2007), pp. 614–620 (cit. on p. 18).
- [28] Porsche. *Panamera S E-Hybrid*. 2015. URL: <http://www.porsche.com/germany/models/panamera/panamera-s-e-hybrid/> (visited on 08/09/2015) (cit. on pp. 6, 7).
- [29] Mark Schudeleit. "Betriebsstrategie für einen parallelen Hybridantrieb." In: *Motortechnische Zeitschrift* (Apr. 2014), pp. 76–83 (cit. on p. 21).
- [30] Toyota. *Prius Plug-in Hybrid*. 2015. URL: <https://www.toyota.at/new-cars/prius-plugin/index.json> (visited on 08/20/2015) (cit. on pp. 9, 10).
- [31] UN. *World population projected to reach 9.6 billion by 2050 – UN report*. 2015. URL: <http://www.un.org/apps/news/story.asp?NewsID=45165> (visited on 08/09/2015) (cit. on p. 1).
- [32] UN. *World Urbanization Prospects: The 2005 Revision*. 2005. URL: <http://www.un.org/esa/population/publications/WUP2005/2005wup.htm> (visited on 08/17/2015) (cit. on p. 1).
- [33] UNECE. *UN Vehicle Regulations - 1958 Agreement*. 2015. URL: <http://www.unece.org/trans/main/wp29/wp29regs101-120.html> (visited on 08/17/2015) (cit. on pp. 7, 27).
- [34] UNECE. *Vehicle Regulations*. 2015. URL: <http://www.unece.org/trans/main/welcwp29.html> (visited on 08/17/2015) (cit. on p. 28).

## Bibliography

- [35] UNECE. *Worldwide harmonized Light vehicles Test Procedure (WLTP)*. 2015. URL: <https://www2.unece.org/wiki/pages/viewpage.action?pageId=2523179> (visited on 08/17/2015) (cit. on p. 28).
- [36] John Wiley and Sons. *Hybrid Electric Vehicles / Principles and Applications with Practical Perspectives*. First Edition. 2011 (cit. on p. 2).
- [37] Karsten Wolter. *Szenarien der Elektromobilität 2050*. first. Thomas Martin Verlagsgesellschaft, 2013. ISBN: 978-3-86924459-4 (cit. on p. 2).
- [38] Mehmet Yay. *Elektromobilität: Theoretische Grundlagen, Herausforderungen sowie Chancen und Risiken der Elektromobilität, diskutiert an den Umsetzungsmöglichkeiten in die Praxis*. second. Peter Lang, 2012. ISBN: 978-3-631-63161-4 (cit. on p. 5).
- [39] ZF. *8HP45 8-Gang-Automatgetriebe für Pkw*. 2015. URL: [http://www.zf.com/media/media/productfinder\\_media/cars/cars\\_driveline\\_8\\_speed\\_automatic\\_transmission/pdf\\_2/8HP45\\_DataSheet.pdf](http://www.zf.com/media/media/productfinder_media/cars/cars_driveline_8_speed_automatic_transmission/pdf_2/8HP45_DataSheet.pdf) (visited on 12/09/2015) (cit. on p. 26).